CH-GFZ-TR-2601

Compact Spherical Coil Calibration

Report and Procedure

	Name	Date and Signature
Prepared by:	H. Lühr, M. Rother, R. Bock (GFZ)	H. Lühr, M. Rother, R. Bock
Checked by:	P. Brauer (DTU-IAU)	22/2-99 Peter Brauer
Project Management:	Prof. Dr. Ch. Reigber (GFZ)	Ch. Reigber

ABSTRACT

This report comprises the results of the performance test conducted with the Fluxgate Compact Spherical Coil (CSC) sensor at the magnetic facility of the Technical University of Braunschweig. Of special interest is the behaviour of the critical parameters over the nominal operation (full performance) temperature range (-20° ... +30°C). During the test the CSC sensors demonstrated their outstanding performances. Subsequently the major results are listed (requirements in parenthesis).

- The noise level within the dynamic range of ±65000 nT was found to be <0.2 nT (0.5 nT).
- There is no indication of a transverse field dependency.
- The temperature coefficient of the scale factors is less than 31 ppm/K (35 ppm/K). The non-linear part is $3.9 \cdot 10^{-8}/K^{-2}$ (linear).
- Temperature dependent offset changes are less than 2 nT (0.5 nT). They can be modelled.
- The temperature dependent change in orientation of the magnetic axes is <2" (5").

All obtained temperature dependent features could be reproduced in a second temperature cycle two days later.

As a by-product it was discovered that the scalar calibration (developed for in-flight calibration) applied to the coil facility did not provide the expected accuracy. A dedicated test of this procedure with CHAMP flight hardware will be performed in the magnetic test facility of the IABG.

Document Change Record

Issue	Date	Page	Description of Change
1.0	05.08.98	all	Draft
1.1	04.02.99	all	First Issue

TABLE OF CONTENT

1 SCOPE

This document comprises the test report and test results obtained during the **Performance Test** of the Fluxgate Magnetometer Compact Spherical Coil (CSC) sensors.

1.1 Test Objective

The objective of this test was to demonstrate the specified performance of CSC sensors, in particular:

a) Orientation of the axes
b) Orthogonality of the system
c) Transverse field dependence of sensitivity
d) Linearity
e) Temperature dependence of sensitivity, offset and orthogonality

The results obtained here will be the basis for the FGM flight data evaluation.

1.2 Test Specimen

The specimen to be tested are the flight hardware FGM sensors including their pigtail harness:

CSC 1	Part-no. CH-11-E-02	Ser.-no.: 0001
CSC 2	Part-no. CH-11-E-03	Ser.-no.: 0002

1.3 Test Date and Location

Date: 23-28 March 1998

Location: Magnetic test facility „Magnetsrode" of the Technical University Braunschweig.

2 DOCUMENTS

The following documents are referred to in this report:

[RD 01] CH-GFZ-SP-0026, issue 1.2
Fluxgate Magnetometer Specification

[RD 02] CH-IGM-TR-0001, issue 1.1
Fluxgate Magnetometer Calibration for CHAMP

[RD 03] CH-IGM-RP-0002, issue 1.1
Magnetsrode: Calibration of the Coil Facility

3 CONDITIONS

3.1 Personnel

The following persons attended the calibration:

Test supervisor	H. Lühr	GFZ
Facility operators	M. Rahm I. Richter	IGM / TUB IGM / TUB
FGM operators	P. Brauer J.M. Garcia-Merayo W. Oelschlägel	IAU / DTU IAU / DTU IAU / DTU
Data analysis	T. Risbo	NBI / KU

3.2 Facilities, Instrumentation and Test Equipment

The calibration was performed in the 2 m coil system of the „Magnetsrode“ magnetic test facility. In the centre of the system the Earth field and its variations are compensated automatically. Artificial fields of up to 100,000 nT in any direction can be generated in the coil system. The field settings can be selected either by hand or computer controlled. In this calibration all tests were run computer controlled using dedicated control files. Field values were randomly distributed to avoid systematic temperature variations.

For monitoring the performance of the facility, temperatures at 64 positions are registered. A description of the facility is given in [RD 03].

The magnetic conditions during the calibration were quiet to moderately active as can be seen from the relevant Kp indices. A recording of the actual magnetic field variations of the days March 23 through 28 is given in [RD 02].

```
YYYYMMDD   Kp [8]                Sum
19980323         0+1-1-1-2-
19980324   0+1-2 2-2+1+2 3       13+
19980325   2+3 1 2+4+5-3-2-      22
19980326   1-2-0+2+4-4 3 2+      18
19980327   3+3-3+3-3 3 3+3-      24
19980328   2+3 2-
```

The units to be calibrated are the FGM flight sensors CSC1 and CSC2. They were operated by an EM DPU. The EGSE consisted of a dedicated power supply and a laptop computer for data read-out.

3.3 Test Software

The software used during the calibration:

DPU software	Mag-Status.vi	version: 1.0	23.03.1998
EGSE software	Read-Mag.vi	version: 1.0	23.03.1998

3.4 Test Conditions

Cleanliness and environmental conditions during the calibration:

<u>Cleanliness:</u> No special requirements since sensors are kept in transport container.

<u>Environmental</u>: The temperature variations at various test points are given in [RD 03].

4 TEST SETUP

The main features of the magnetic facility are given in [RD 02]. It should just be mentioned here that the coil system is located in the non-magnetic House 2 and control electronics is installed in House 1, some 30 m apart.

The magnetometers to be tested were set up as illustrated in *Figure 4-1.*

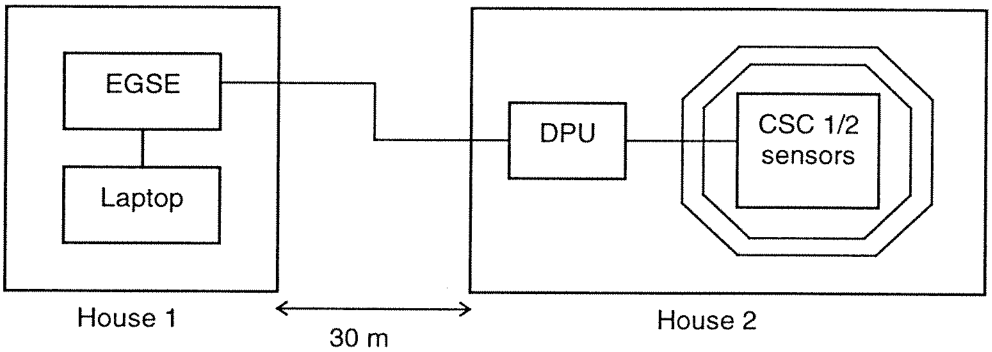

Figure 4-1 Test set-up for CSC 1/2 calibration

5 SEQUENCE OF TESTS STEPS

During the week March 23-28, 1998 the following measurements were performed:

Monday March 23, 1998							
Test No.	**Start Time, UT**	**Sensor**	**Axes Orientation**			**No. of settings**	**Field strength, µT**
			North	**East**	**Zenith**		
–		Setup of measurement equipment					
–	10:49	Coil calibration with GEM Overhauser at 50 µT					
–	11:44	Coil calibration with GEM Overhauser at 30 µT					
–	13:52	Check of the CSC 1/2 axes assignments					
1	14:23	CSC 1	+X	+Y	+Z	83	30
2	16:08	CSC 1	+X	+Y	+Z	83	30
3	17:05	CSC 1	+X	+Y	+Z	83	45
4	18:02	CSC 1	+X	+Y	+Z	83	60
5	19:18	CSC 1	-Y	+X	+Z	83	30
6	20:15	CSC 1	-Y	+X	+Z	83	45
7	21:12	CSC 1	-Y	+X	+Z	83	60
8	22:08	CSC 1	-Y	+X	+Z	688	50

Tuesday March 24, 1998

Test No.	Start Time, UT	Sensor	Axes Orientation North	East	Zenith	No. of settings	Field strength, µT
9	06:00	CSC 1	-Z	+Y	+X	83	30
10	06:56	CSC 1	-Z	+Y	+X	83	45
11	07:53	CSC 1	-Z	+Y	+X	83	60
12	08:50	CSC 1	-Z	+Y	+X	116	50
13	11:51	CSC 1	-Y	+X	+Z	2170	50

Wednesday March 25, 1998

Test No.	Start Time, UT	Sensor	Axes Orientation North	East	Zenith	No. of settings	Field strength, µT
–	12:24	Coil calibration with GEM Overhauser at 30 µT					
14	13:48	CSC 2	+X	+Y	+Z	1771	50

Thursday March 26, 1998

Test No.	Start Time, UT	Sensor	Axes Orientation North	East	Zenith	No. of settings	Field strength, µT
15	09:53	CSC 2	+X	+Y	+Z	161	64
16	13:01	CSC 1	-Z	+X	-Y	1823	50

Friday March 27, 1998

Test No.	Start Time, UT	Sensor	Axes Orientation North	East	Zenith	No. of settings	Field strength, µT
17	09:21	CSC 1	-Z	+X	-Y	162	64
–	11:22	Coil calibration with GEM Overhauser at 50 µT					
18	12:39	CSC 2	skewed 45 deg.			100	65
19	14:49	CSC EM	+X	+Y	+Z	ca. 1600	50

Saturday March 28, 1998

–	10:00	Packing and departure

6 CHARACTERISTICS OF THE COIL FACILITY

The main parameters of the coil system were determined repeatedly with the help of a GEM Overhauser magnetometer. In section 5 these test steps are labelled 'coil calibration'. The results are:

Scale factor in nT/EU

Date	Time	F_X	F_Y	F_Z	T_X	T_Y	T_Z
23.03.98	10:49	0.999879	0.999934	0.999942	16.56	16.50	16.60
23.03.98	11:44	0.999883	0.999935	0.999945	16.38	16.32	16.35
25.03.98	12:24	0.999882	0.999925	0.999930	16.60	16.56	16.55
27.03.98	11:22	0.999860	0.999916	0.999920	17.03	16.96	17.03

Field Offset in nT

Date	Time	O_X	O_Y	O_Z	T_X	T_Y	T_Z
23.03.98	10:49	2.07	-2.08	-1.14	16.56	16.50	16.60
23.03.98	11:44	1.92	-2.42	-1.27	16.38	16.32	16.35
25.03.98	12:24	2.41	-4.49	-0.01	16.60	16.56	16.55
27.03.98	11:22	1.41	-4.45	-2.57	17.03	16.96	17.03

Angles between components in degrees

Date	Time	(X/Y)	(X/Z)	(Y/Z)	T_X	T_Y	T_Z
23.03.98	10:49	90.0029	89.9961	89.9663	16.56	16.50	16.60
23.03.98	11:44	90.0033	89.9964	89.9664	16.38	16.32	16.35
25.03.98	12:24	90.0029	89.9960	89.9666	16.60	16.56	16.55
27.03.98	11:22	90.0033	89.9963	89.9651	17.03	16.96	17.03

From [RD 03] it is known that some of the coil system parameters (scale factor, offset) are temperature dependent. When taking this into account we have identified a set of coil system parameters, which are valid for this calibration. The 'coil calibration' on March 27 showed increased residuals and is thus considered with a lower weight.

Scale factors in nT/EU

$$F_X = 0.999\,88 \cdot [1+0.0000190\,(T_X - 16.5)]$$

$$F_Y = 0.999\,93 \cdot [1+0.0000165\,(T_Y - 16.5)]$$

$$F_Z = 0.999\,94 \cdot [1+0.0000175\,(T_Z - 16.5)]$$

Offset fields in nT

(valid March 23-25, 12:00 UT)

$0_X = 2.0 + 0.35\,(T_X - 16.5)$

$0_Y = -2.2$

$0_Z = -1.2 + 0.80\,(T_Z - 16.5)$

(valid March 25-28, 12:00 UT)

$0_X = 2.0 + 0.35\,(T_X - 16.5)$

$0_Y = -4.4$

$0_Z = -1.2 + 0.80\,(T_Z - 16.5)$

Angels between components in degree

(X,Y) = 90.0031
(X,Z) = 89.9962
(Y,Z) = 89.9664

The behaviour of the coil temperatures T_X, T_Y and T_Z is plotted in [RD 03] and labelled there TCA_X, TCA_Y and TCA_Z, respectively.

During the course of data evaluation it became clear that there is a certain dependency of the field settings on the temperature in House 1 where the control electronics is installed. We used the long-time over-night run No. 8 for a consistency check of the estimated values.

Final scale factors in nT/EU

$F_{XX} = F_X\,[1 - 8 \cdot 10^{-7}\,(T_R - 32)]$
$F_{YY} = F_Y\,[1 - 8 \cdot 10^{-7}\,(T_R - 32)]$
$F_{ZZ} = F_Z\,[1 - 8 \cdot 10^{-7}\,(T_R - 32)]$

Final offset fields in nT

$0_{XX} = 0_X + 0.075 \cdot (T_R - 32)$
$0_{YY} = 0_Y$
$0_{ZZ} = 0_Z + 0.2 \cdot (T_R - 32)$

The temperature T_R is taken in the electronics rack of the facility control electronics in House 1. In [RD 03] this temperature is labelled T_{55} and its variations are plotted.

There are no dependencies of the facility axes orientation on temperatures.

7 MEASUREMENTS AT AMBIENT TEMPERATURE

In the beginning a number of measurements were made at ambient temperature which should help to assess the quality and reproducibility of the results. Particularly instructive in this respect is the long night run No. 8. With its duration of 8 hours it can be regarded as a test of the system stability and as a verification of the temperature corrections applied to the coil facility.

When interpreting the raw data from the magnetometer we found that the readings showed a slight non-linear effect. With the help of a third order polynom the data could be linearised. The same polynom as determined from run No. 8 was used to correct all the measurements made during this test. The actual coefficients are of no concern here, since the non-linearity is caused by the analogue-to-digital converter (ADC) and the unit used in this test was the EM. It will be part of the overall magnetometry package calibration at IABG to determine the linearisation coefficients for the two flight units.

Figure 7-1 shows the residuals versus time obtained after a linear regression between field settings and magnetometer readings (all corrections mentioned in section 6 have been applied). There are a few things worth mentioning. The residuals are confined to a band of about ±0.2 nT. The obtained standard deviations ($\sigma \approx 0.14$ nT) comprises the noise of the facility plus the magnetometer. There are somewhat larger undulations in the sensor X component. These are most probably caused by variations in the facility. Also during other measurements the facility Y component tended to be less stable. The absence of a trend in the residuals proves the validity of the applied corrections and the stability of the system.

In Figure 7-2 the residuals are presented in a somewhat different perspective. Now the dependence on the applied field is of interest. The nine frames comprise all possible combinations between the three facility and the three sensor axes. In general we get the same result as before. The residuals are limited to a band of ±0.2 nT except for the sensor X component, as discussed before. There is no obvious non-linear relationship between any of the facility axes and the sensor axes. When taking a close look a tiny systematic dependence of about ±0.2 nT seems to exist between sensor X and facility Y @ 40 μT, sensor Y and facility X @ -40 μT, and sensor Z and facility Z @ 40 μT. Considering the orientation of the sensor axes in the coil facility during run No. 8, as stated in section 5, we see that this small deviation appears in all cases in the on-axis component at field strengths around +40 μT. This effect is again attributed to the ADC and has to be addressed during the IABG calibration. Finally it should be stressed that the CSC sensors do not show any dependencies on fields perpendicular to the measurement direction.

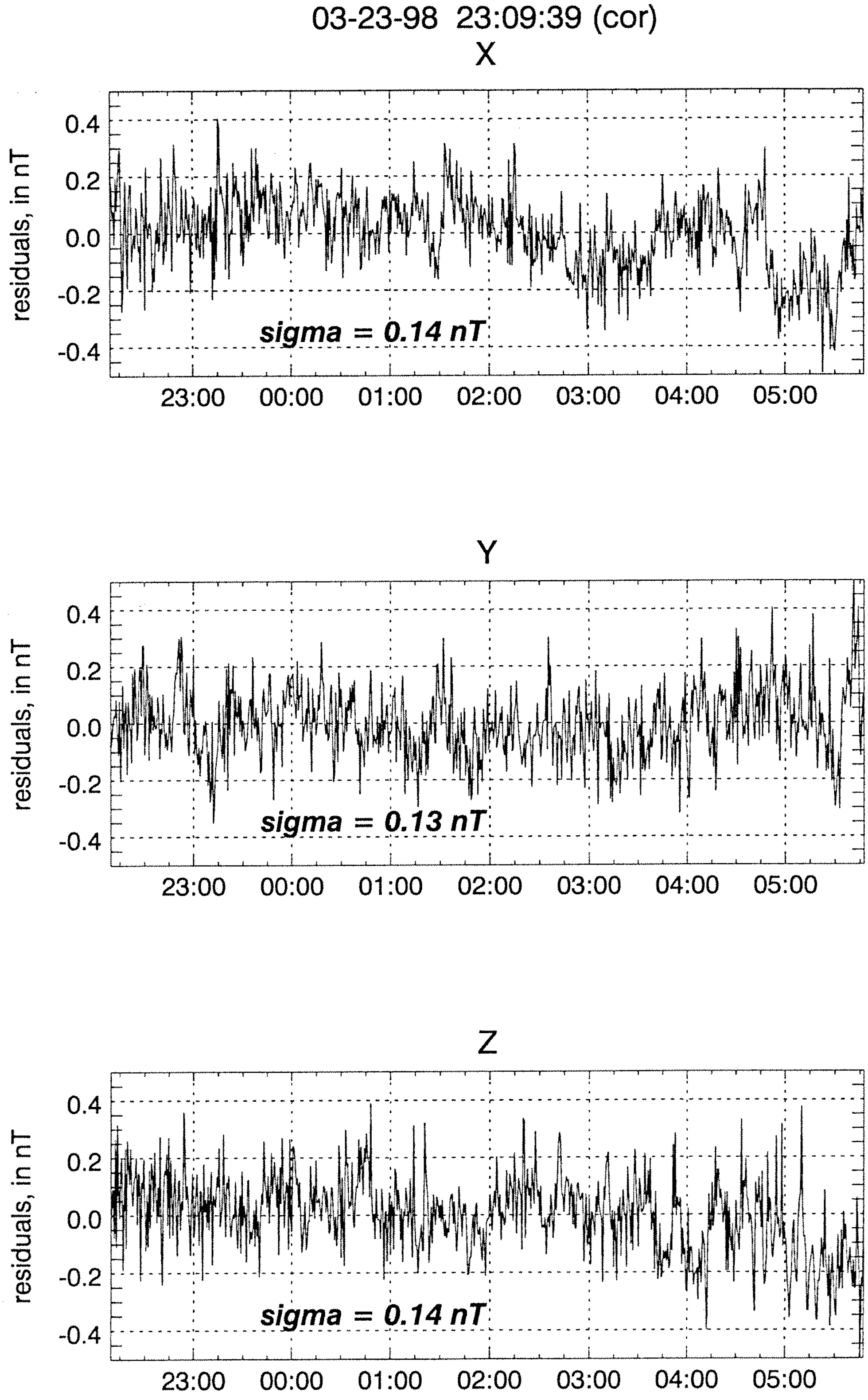

Figure 7-1 Residuals versus time

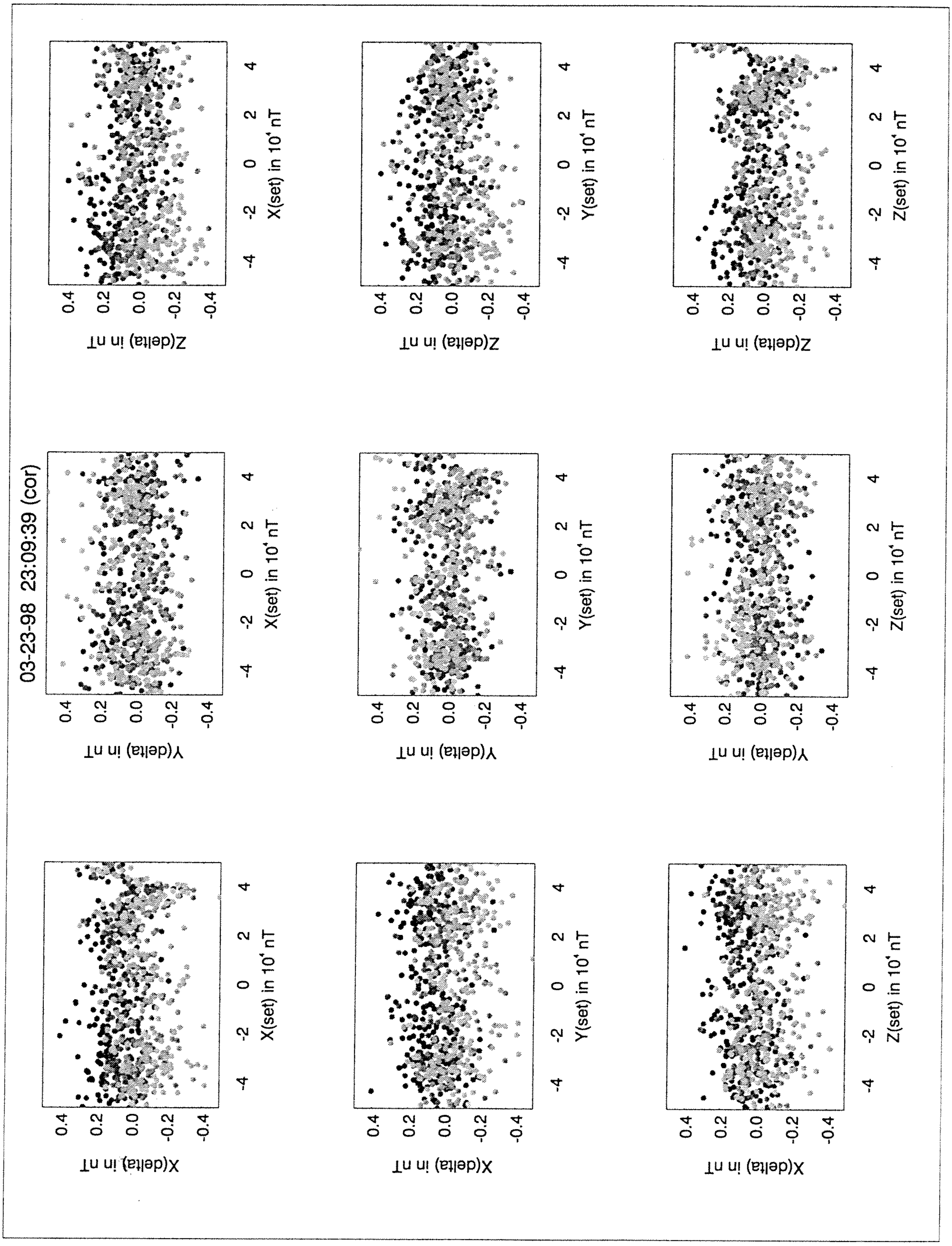

Figure 7-2 Residuals versus applied fields

A whole series of runs has been performed just to check the repeatability of results and to find persistent features. Below results are sorted by the three sensor parameters. As an example for the quality of the measurement a complete listing of run No. 4 is added in Appendix A.

The features of a triaxial sensor are characterised by 9 parameters: sensitivity, offset and misalignment for each axis.

Sensitivity (nT/EU), CSC 1

Run No.	No. of settings	Field strength, µT	S_X	S_Y	S_Z
1	83	30	0.998942	1.001765	0.999322
2	83	30	0.998944	1.001763	0.999320
3	83	45	0.998944	1.001765	0.999323
4	83	60	0.998943	1.001764	0.999318
5	83	30	0.998964	1.001741	0.999308
6	83	45	0.998965	1.001742	0.999309
7	83	60	0.998964	1.001742	0.999307
8	688	50	0.998964	1.001742	0.999306
9	83	30	0.998932	1.001760	0.999334
10	83	45	0.998934	1.001762	0.999336
11	83	60	0.998935	1.001762	0.999332
12	116	50	0.998933	1.001765	0.999333
17	162	64	0.998947	1.001745	0.999320
CSC 2					
15	161	64	0.998622	1.002611	0.999040
18	100	64	0.998630	1.002617	0.999034

Offset (nT) and misalignment (deg), CSC 1

Run No.	X_0	Y_0	Z_0	(X/Y)	(X/Z)	(Y/Z)
1	-169.3	-159.4	-77.3	89.9738	89.9354	89.9611
2	-165.6	-157.6	-76.9	89.9736	89.9353	89.9609
3	-165.8	-157.6	-77.3	89.9736	89.9353	89.9610
4	-165.7	-157.6	-77.5	89.9736	89.9353	89.9610
5	-165.8	-151.9	-77.1	89.9756	89.9377	89.9631
6	-165.8	-151.9	-77.3	89.9754	89.9378	89.9630
7	-165.8	-151.9	-77.6	89.9754	89.9378	89.9631
8	-165.8	-152.0	-77.8	89.9755	89.9378	89.9631
9	-169.9	-157.0	-67.9	89.9739	89.9398	89.9627
10	-170.0	-157.0	-68.2	89.9740	89.9398	89.9627
11	-170.1	-156.9	-68.6	89.9740	89.9398	89.9628
12	-170.3	-157.1	-68.4	89.9741	89.9398	89.9628
17	-165.1	-157.0	-71.9	89.9744	89.9370	89.9609
CSC 2						
15	-167.9	-171.1	-65.5	89.9350	90.0309	89.9174
18	-166.8	-170.2	-68.3	89.9345	90.0313	89.9169

The 13 runs performed with CSC 1 can be divided in four groups. For each of the groups the orientation of the CSC sensor with respect to the facility axes was changed (cf. section 5). Within a group the results are very consistent. There is no dependence on the applied field strength or the number of readings. When, however, comparing different groups, significant differences are apparent especially in the offsets and the misalignment angles. A possible explanation would be that the sensor locations were a little bit different for each of the groups. It is unlikely that this was the cause, since (1) we used a laser beam to ensure a correct positioning to about 1 mm and (2) results are constant across group boundaries for sensor axes which have not changed their orientation with respect to the facility axes (cf. Offset Y_0: Group 1 and 3, Offset Z_0: Group 1 and 2). This result suggests that the calibration of the facility with the GEM Overhauser is not fully correct. When adjusting the sensitivity by about 10 ppm, the offsets by a few nT and the facility angles by some 5 arcsec we can obtain consistent results for all runs. A possible reason for this discrepancy could be a heading error at the GEM sensor. Special attention has to be paid to this effect during the IABG magnetic test to make sure that the LETI Overhauser sensor to fly on CHAMP does not suffer from this deficiency.

The CSC 2 sensor was less thoroughly tested, since CSC 1 will be the main sensor for the Fluxgate measurements. The two measurements at ambient temperature (before and after the temperature run) gave very much the same results.

8 TEMPERATURE DEPENDENCE OF THE CSC SENSORS

The most important part of the sensors calibration was to determine their dependence on temperature variations. As listed in section 5 two thermal cycles were performed with CSC 1 and one with CSC 2. The two thermal cycles of CSC 1 were two days apart and the orientation of the sensor was different in the two cases to allow for separation between effects caused by the facility and the sensor.

For this test the non-magnetic thermal box of the facility was used. Cooling was facilitated by adding dry ice (solid CO_2) and heating by short electric pulses outside the measurement periods. The temperature range covered extended from -40°C to 30°C.

Figure 8-1 depicts the variation of the sensor temperature during the three tests. During the cooling phase and the first recovery the temperature was passively following the conditions given by the evaporating dry ice. Above 0°C a controlled heating with a rate of 5 K/hour was applied.

There are two curves in Figure 8-1. The one labelled T_{sens} represents the temperature of the inner ring core elements and T_{CSC} tracks the temperature of the spherical shell. T_{sens} is always higher than T_{CSC} indicating that there is a net heat flow from the centre to the surface.

From Figure 8-2 it can be seen that the temperature difference between the two measurement points depends on the change rate of the ambient temperature. We obtain a more or less linear relation between temperature difference and the change rate if the variations are not too rapid. This dependency can be interpreted in terms of differences in thermal time constants for the two temperature readings. A linear regression gives the following results:

$$\text{CSC1:} \quad T_{CSC} - T_{sens} = 15.4\ dT/dt - 2.1\ K$$

$$\text{CSC2:} \quad T_{CSC} - T_{sens} = 17.5\ dT/dt - 2.4\ K$$

where the time t is measured in minutes. These equations tell us that T_{sens} is about 2 K higher than T_{CSC} and T_{sens} senses the ambient temperature 15.5 and 17.5 min later than T_{CSC} for the CSC1 and CSC2 sensors, respectively. In case the T_{CSC} measurements have to be replaced by T_{sens}, the above relation has to be taken into account. In all subsequent evaluations we will use only T_{CSC}.

The features of a triaxial sensor are characterised by 9 parameters as mentioned before. In the following we will have a look at the temperature dependence of these parameters. During all the temperature cycles the magnetometer was operated and magnetic fields with a constant amplitude of 50,000 nT but randomly distributed direction were applied by the facility. Settings were changed every 40 sec. For the determination of the nine sensor parameters 18 settings were used resulting in an ensemble average over 12 min. Such a sliding window was moved over the whole data set.

As an example for the quality of the results Figure 8-3 depicts the sensitivity dependence on temperature. The curve shows a hysteresis effect. The upper branch results from the rapid temperature descent in the beginning of the cycle. This part of the data has not been taken into account for the determination of the final coefficients since the system was not in thermal equilibrium during that time. Supporting evidence for this decision comes from the obtained residuals, as shown in Figure 8-4. During the early phase with high change rates the spread is large. It decreases as the temperature varies more gradually (cf. Figure 8-1). In the sensor Z component the standard deviation is slightly elevated. We attribute this again to the facility Y component which has been identified earlier as a little more noisy.

The hysteresis effect clearly recognisable in Figure 8-3 is caused by a delayed response of the feed back coils on the CSC with respect to the readings of T_{CSC}. If we are again assume not too rapid temperature changes, we may use a constant lead time for the T_{CSC} readings, as we suggested it for the difference between T_{CSC} and T_{sens}. The best match between the cooling and heating branch is obtained when allowing for a latency of 8 minutes for the CSC1 and CSC2 sensor feed back coils. Figures 8-5 and 8-6 show the improved sensitivity dependence on temperature of CSC1 and CSC2 when the above noted delay time is taken into account.

In Appendix B sensitivity curves versus T_{sens} are shown. Here we find a hysteresis effect with the opposite sense. If we now delay the T_{sens} readings by 8 min the heating and cooling branches are matching.

The variation of the nine sensor parameters caused by the changing temperature is shown for CSC 1 in Figures 8-7 through 8-12 and for CSC 2 in Figures 8-13 through 8-15. In case of CSC 1 we take advantage of the two independent thermal cycles to check the reliability of the results. Figures 8-7 and 8-8 show the behaviour of the offsets. From the comparison between cycle 1 and 2 we can deduce that the sensor X component shows virtually no dependence on temperature. For the Y component we find a slight decrease in offset at a rate of about 0.5 nT per 10 K for temperatures below -10 °C. At higher temperatures no noticeable dependence is found. In case of the Z component both cycles reveal an anti-correlation between temperature and offset with an average slope of -0.04 nT/K.

The dependence of the sensitivity on temperature is shown in Figures 8-9 and 8-10. The sensitivity slopes off with about 30 ppm/K over the whole temperature range. The measurements from the two cycles give almost identical results. There is a small but consistent quadratic term of $-3.8\ 10^{-8}/K^2$ apparent in all curves.

The behaviour of the angles between the sensor axes over the specified temperature range is shown in Figures 8-11 and 8-12. Here again the outstanding stability features of the CSC sensors are apparent. When comparing the results of the two thermal cycles no noticeable trend in the arc second range was observed for the two angles (X,Y) and (Y,Z). A tiny but consistent negative correlation of $-1.3\ 10^{-5}$ deg/K shows up in the angle (X,Z).

Very much comparable results were obtained for the sensor CSC2. This sensor was subjected only to a single temperature cycle. The high degree of reproducibility experienced with CSC1 is supporting the reliability of the results. The offsets shown in Figure 8-13 exhibit little dependency on temperature. In case of the X and Z components the variations are limited to a 1 nT band. Only the Y component shows a noticeable trend of -0.05 nT/K on average.

The sensitivity again follows the temperature with a slope of about $-30\ 10^{-6}/K$ (see Figure 8-14) much the same as obtained for the sensor CSC1. A quadratic term of $-3.9\ 10^{-8}/K^2$ is attributed to all three components.

In case of the angles between the components, as shown in Figure 8-15, none of the angles exhibit a recognisable trend.

All these data show the high reliability of the results obtained during the thermal cycling and the outstanding performance of the CSC sensors over a wide temperature range.

For completeness we have added curves of the sensitivity versus T_{sens} in Appendix B. In case T_{CSC} fails the scale factors can be corrected with the readings of this thermistor. In all these graphs the temperature readings have been advanced by 8 min.

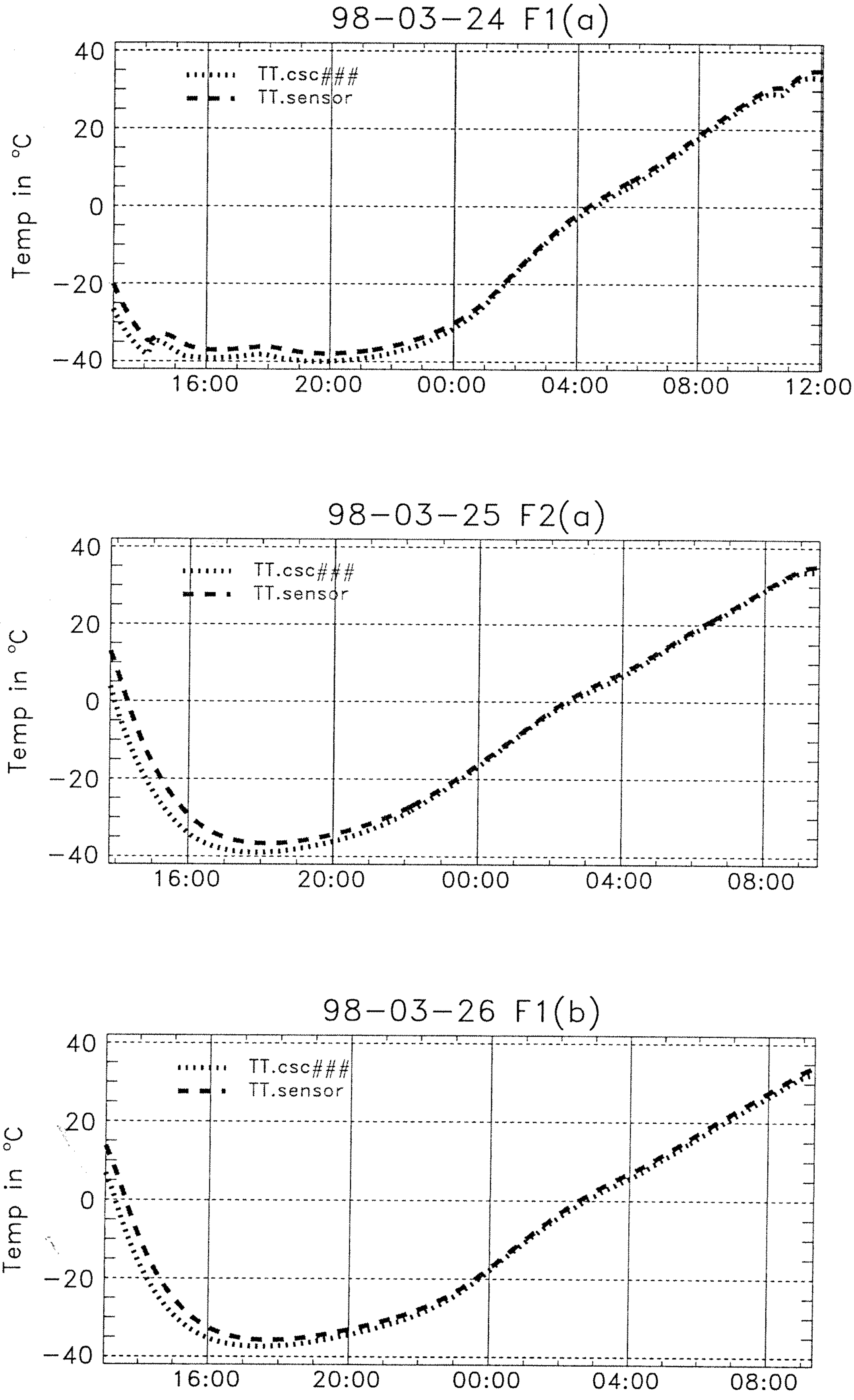

Figure 8-1 Sensor temperature during thermal cycles

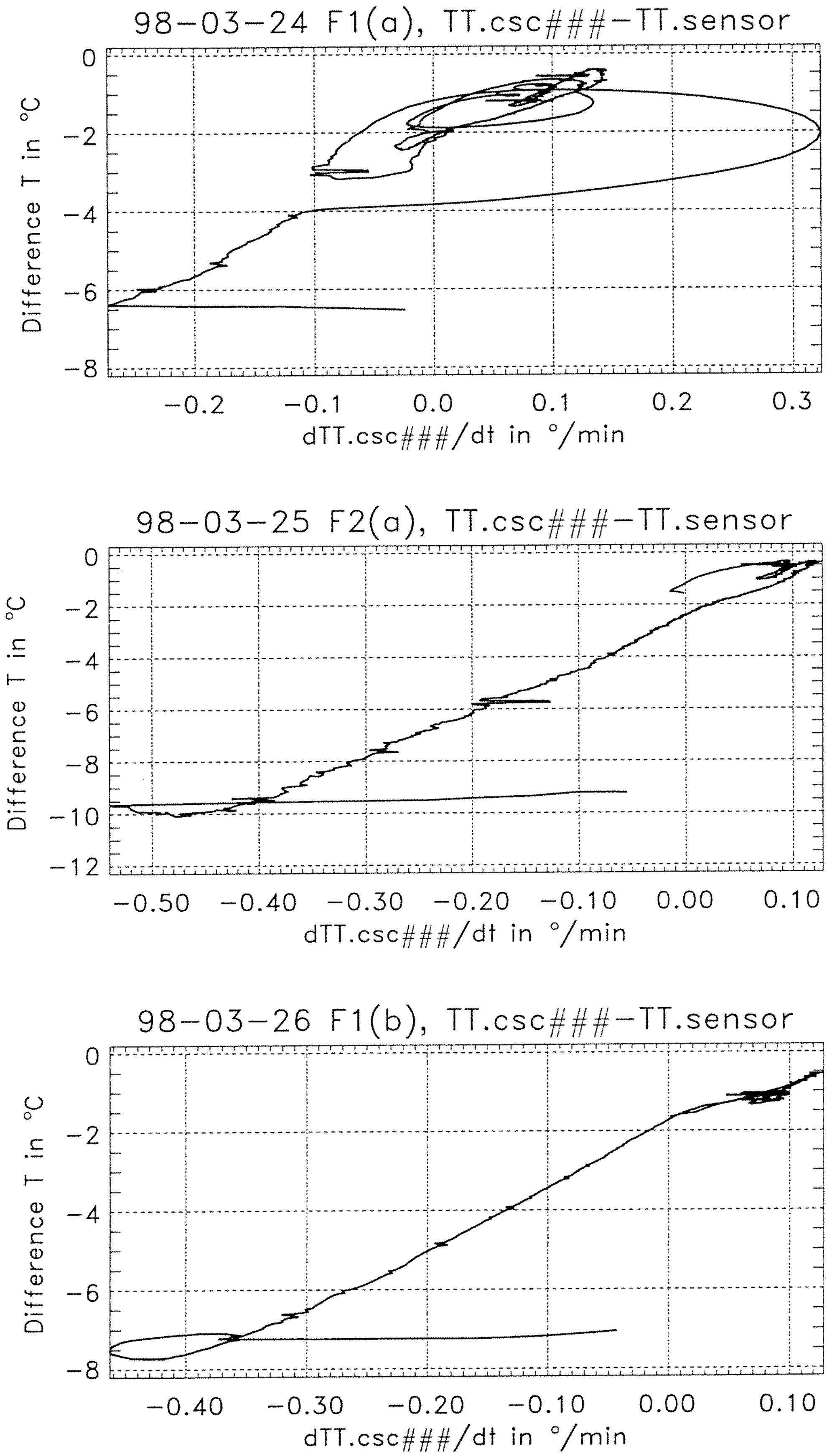

Figure 8-2 *Difference of the two thermistor readings versus change rate*

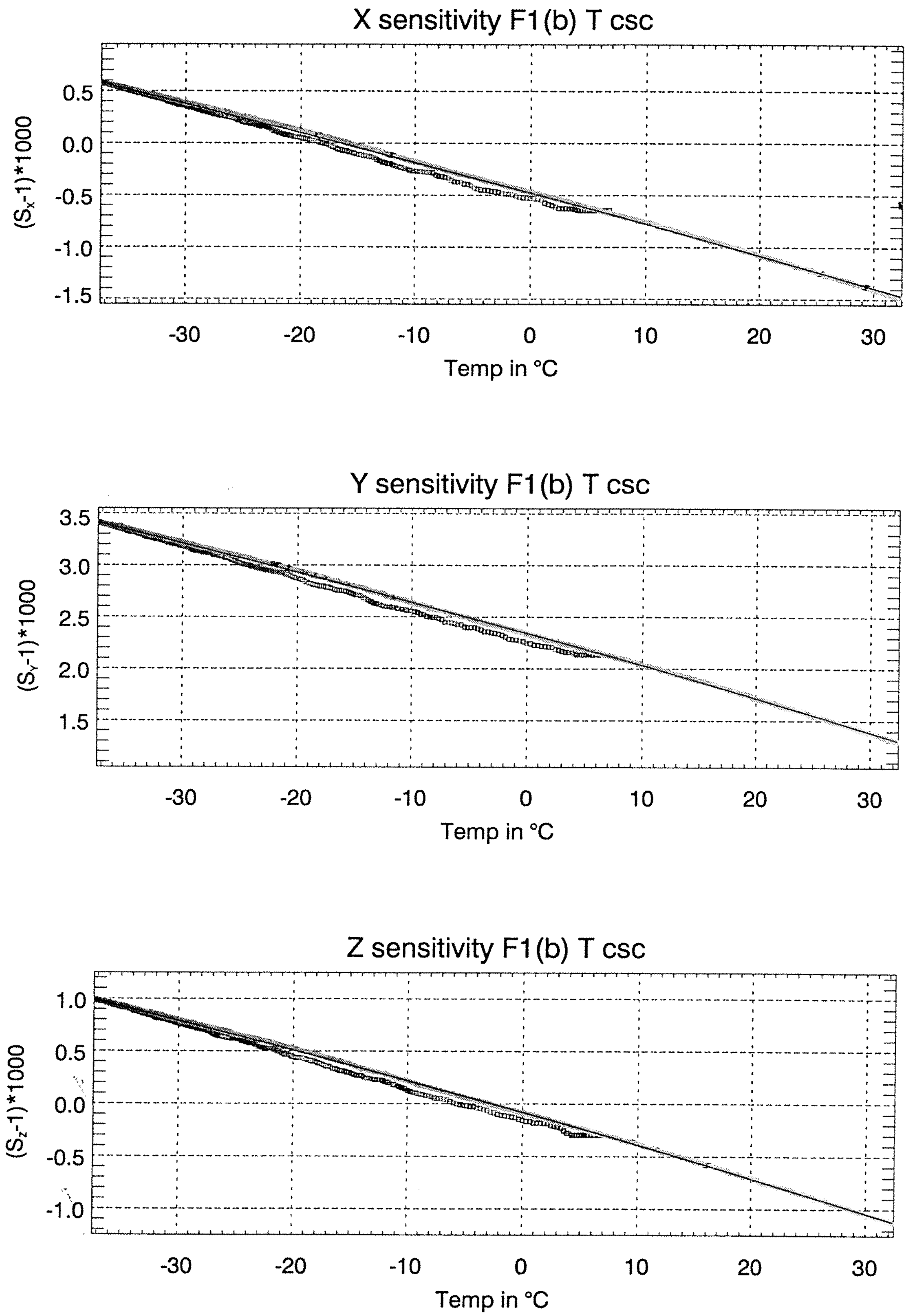

Figure 8-3 Change of scale factor versus temperature (T_{CSC})

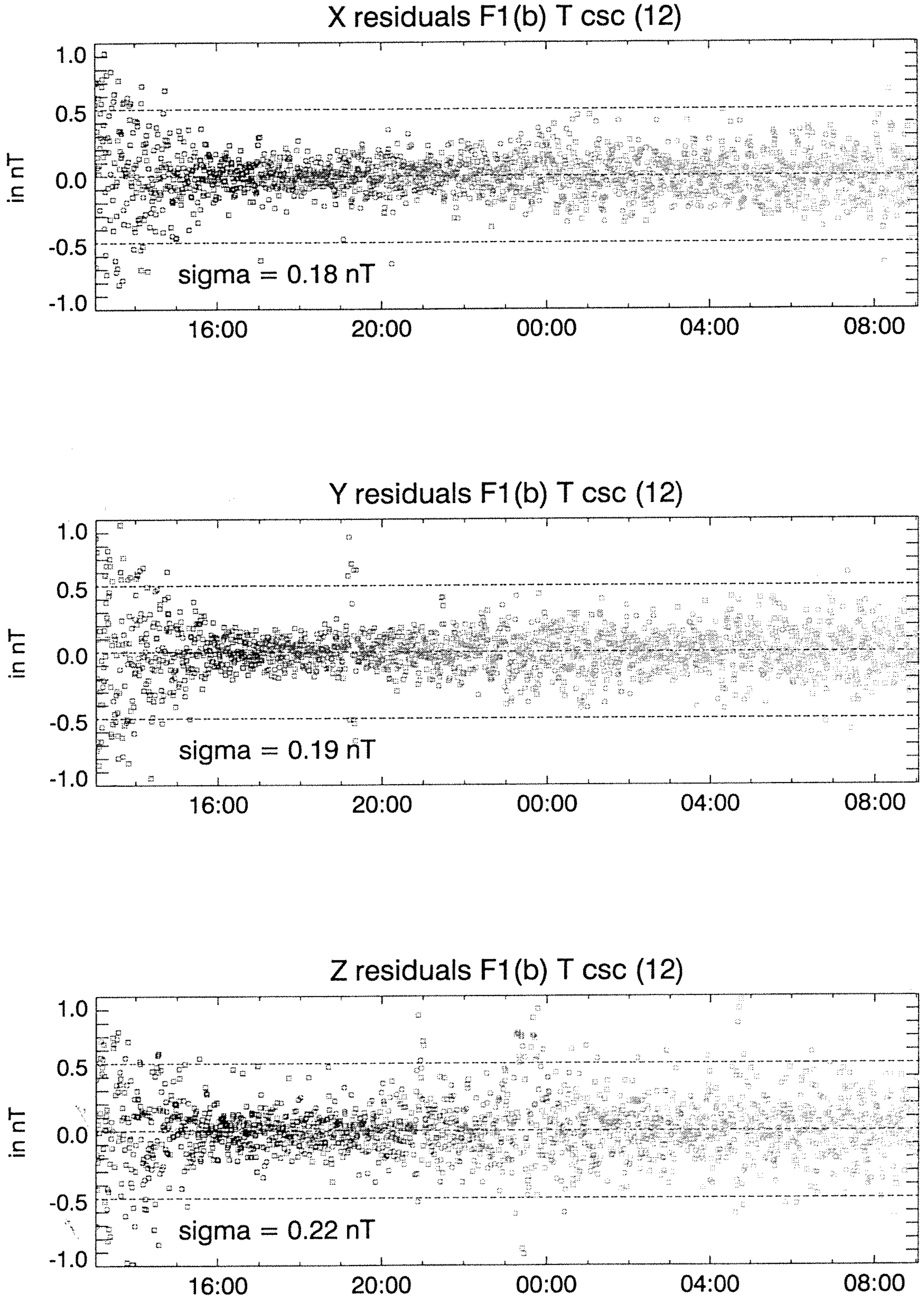

Figure 8-4 Residuals obtained during thermal cycle

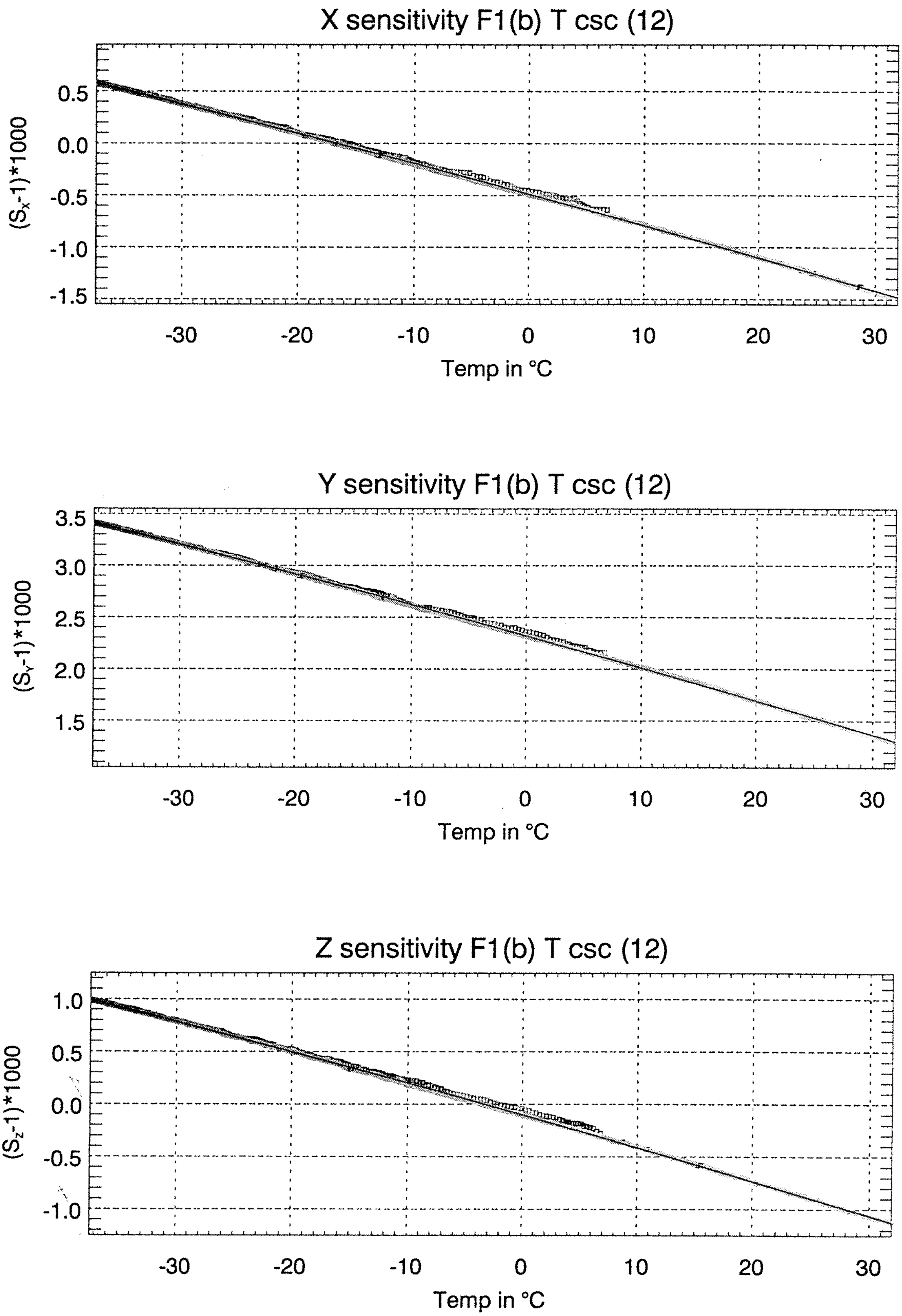

Figure 8-5 *CSC 1 , change of scale factor versus temperatures; T_{CSC} readings delayed by 8 min.*

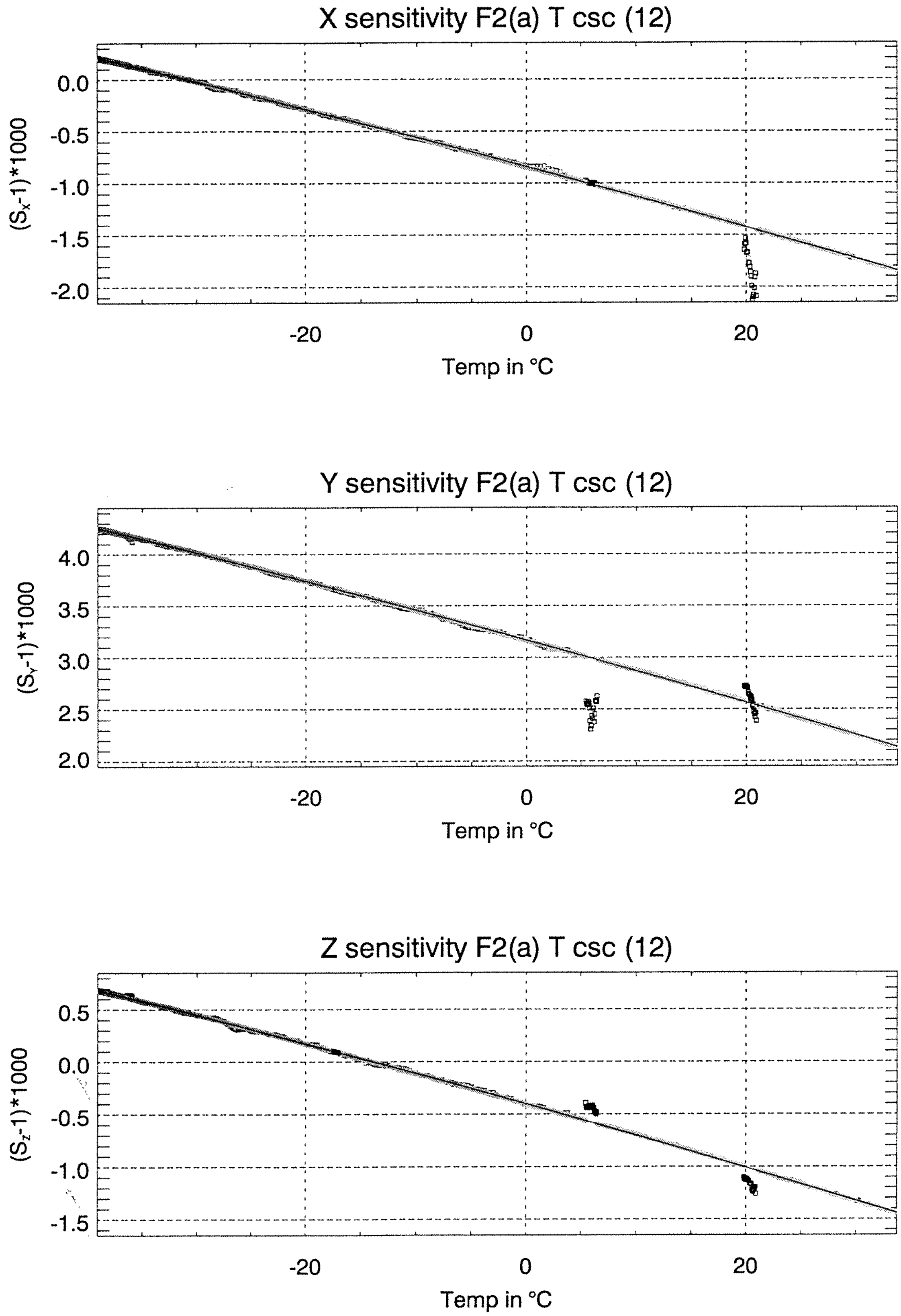

Figure 8-6 *CSC 2 , change of scale factor versus temperatures; T_{CSC} readings delayed by 8 min.*

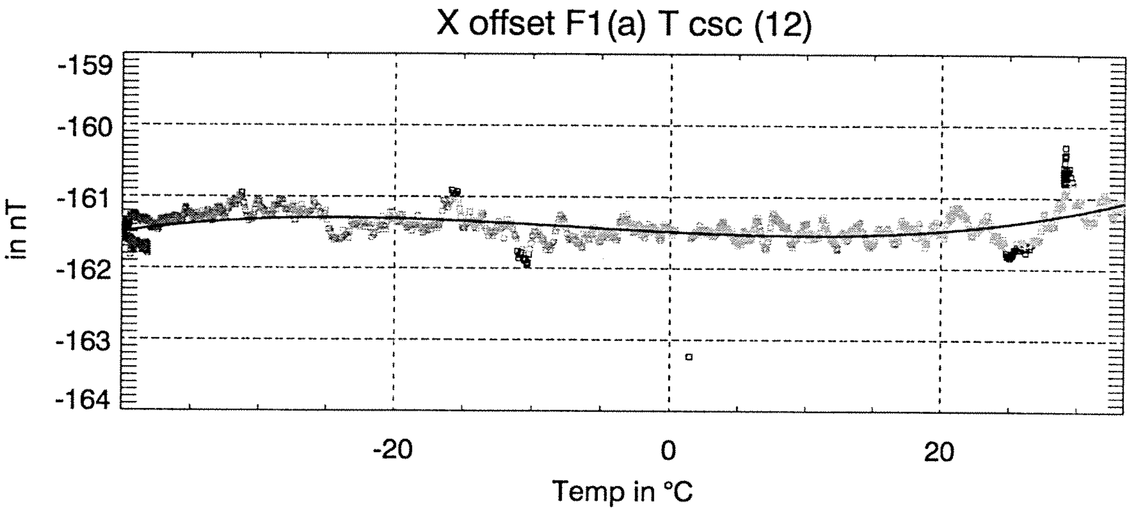

(400), -161.48772 -0.0088819413 0.00024807416 1.1863549e-05

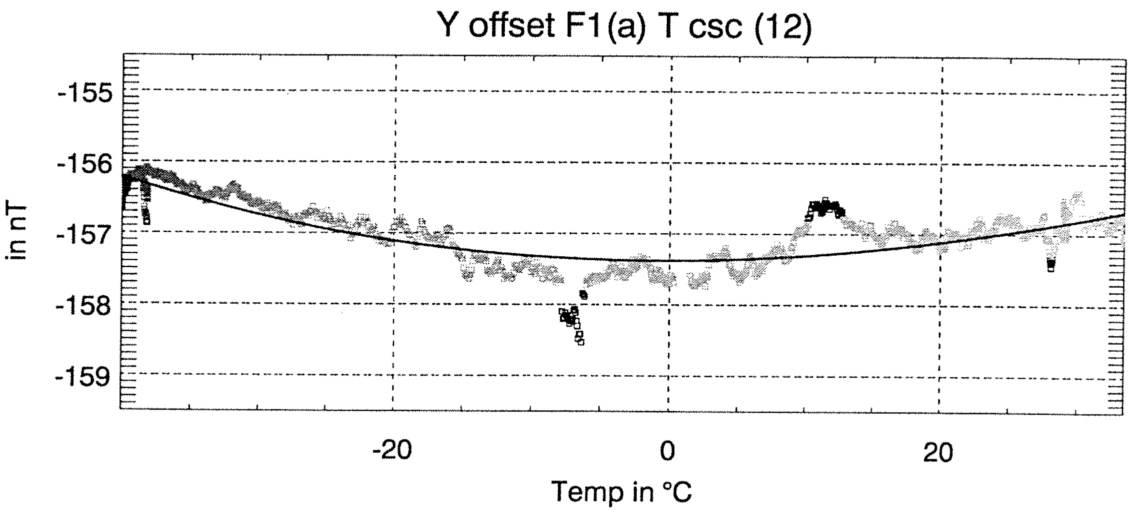

(400), -157.37807 0.00064995940 0.00066940515 -1.9559029e-06

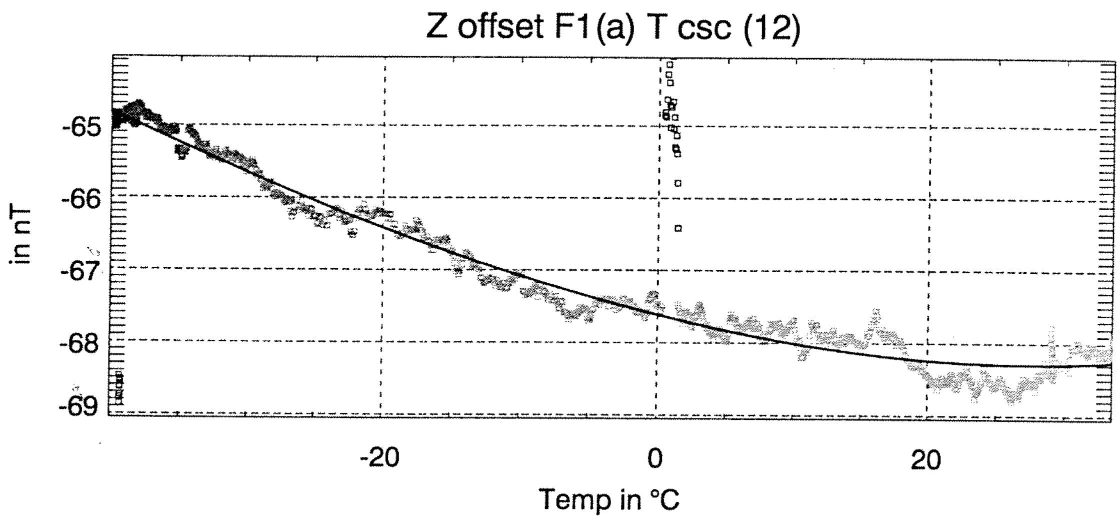

(400), -67.612578 -0.046783112 0.00071259473 3.3228705e-06

Figure 8-7 CSC 1 , change of offsets versus temperature

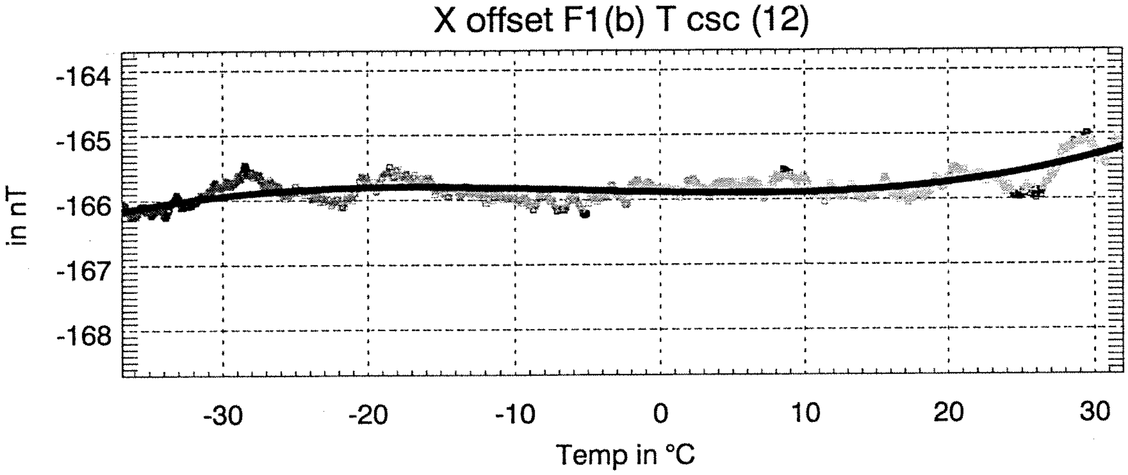

(500), -165.88083 -0.0051491707 0.00027746172 1.7058076e-05

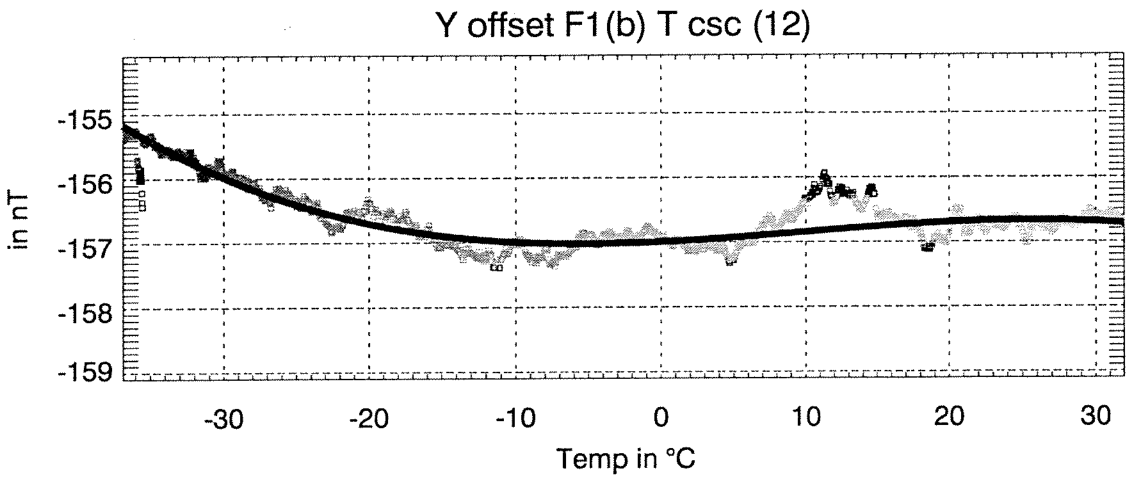

(500), -156.98943 0.0099180498 0.00072536887 -2.4083483e-05

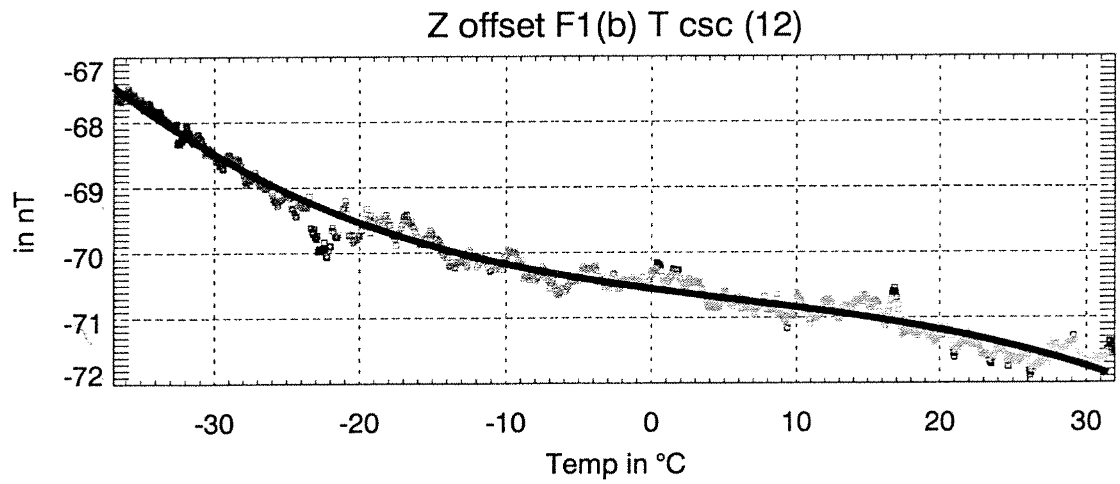

(500), -70.553938 -0.030644696 0.00048527950 -2.6292284e-05

Figure 8-8 CSC 1 , change of offsets versus temperature

X sensitivity F1(a) T csc (12)

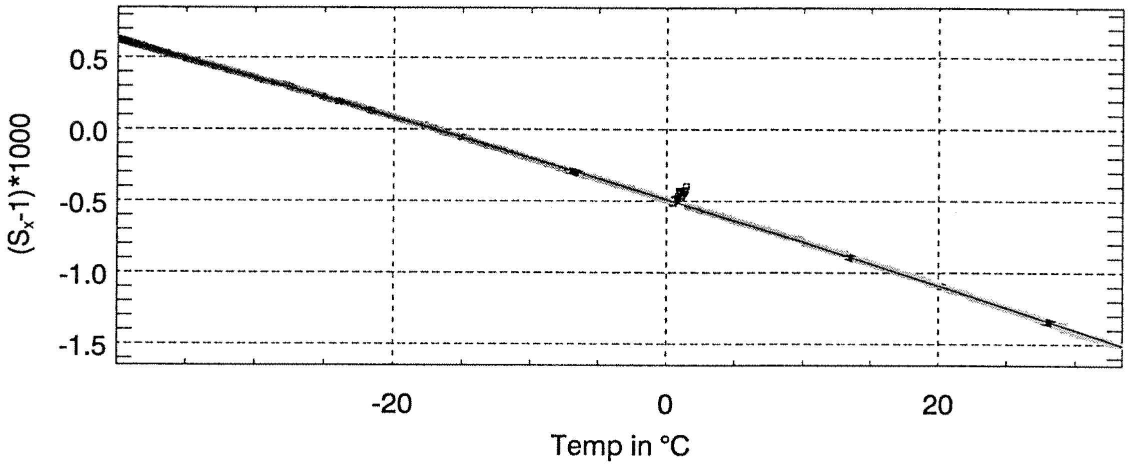

(400), 0.99951067 -2.9348735e-05 -3.6240859e-08

Y sensitivity F1(a) T csc (12)

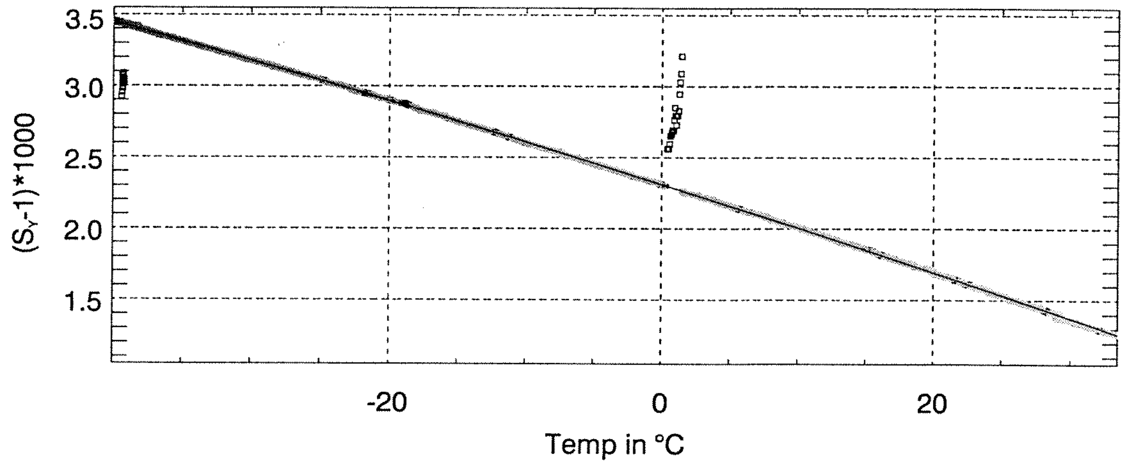

(400), 1.0023110 -3.0126675e-05 -3.8002948e-08

Z sensitivity F1(a) T csc (12)

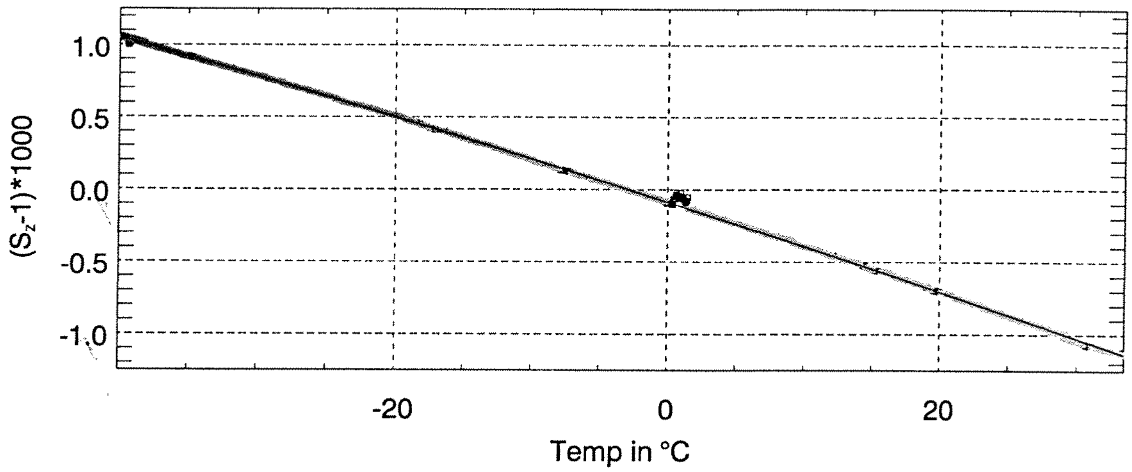

(400), 0.99991232 -3.0149443e-05 -3.8251802e-08

Figure 8-9 CSC 1 , temperature dependence of scale factor

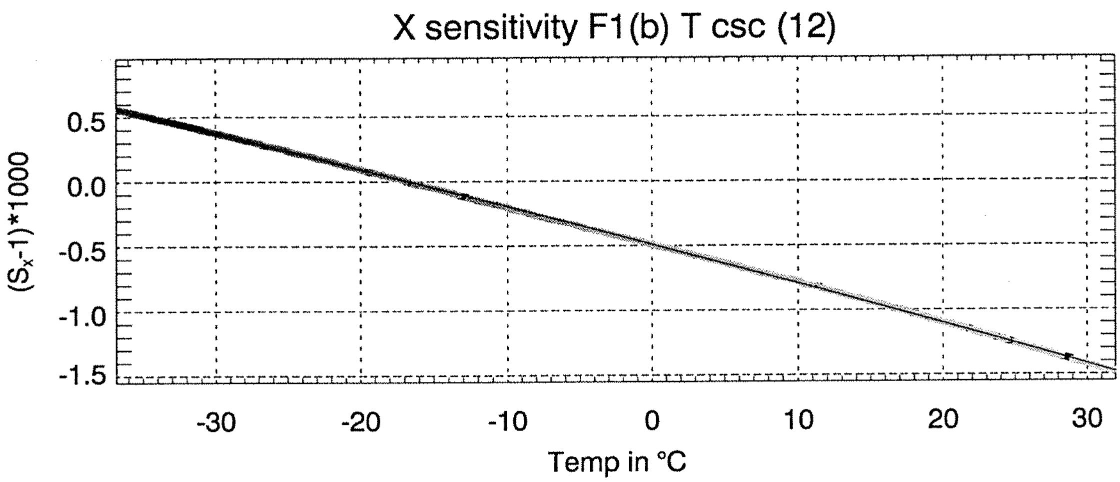

(500), 0.99951080 -2.9848009e-05 -3.5301105e-08

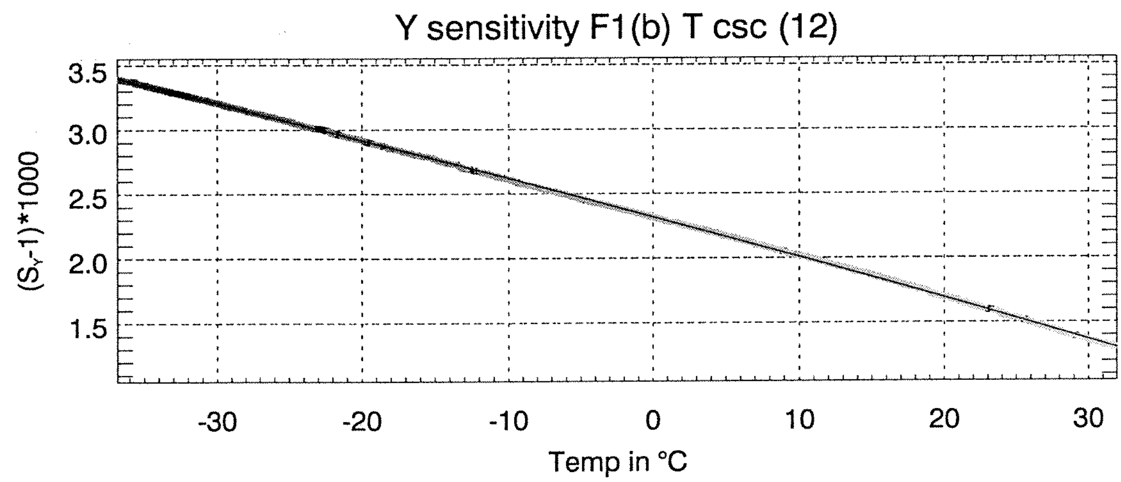

(500), 1.0023193 -3.0604868e-05 -3.6868521e-08

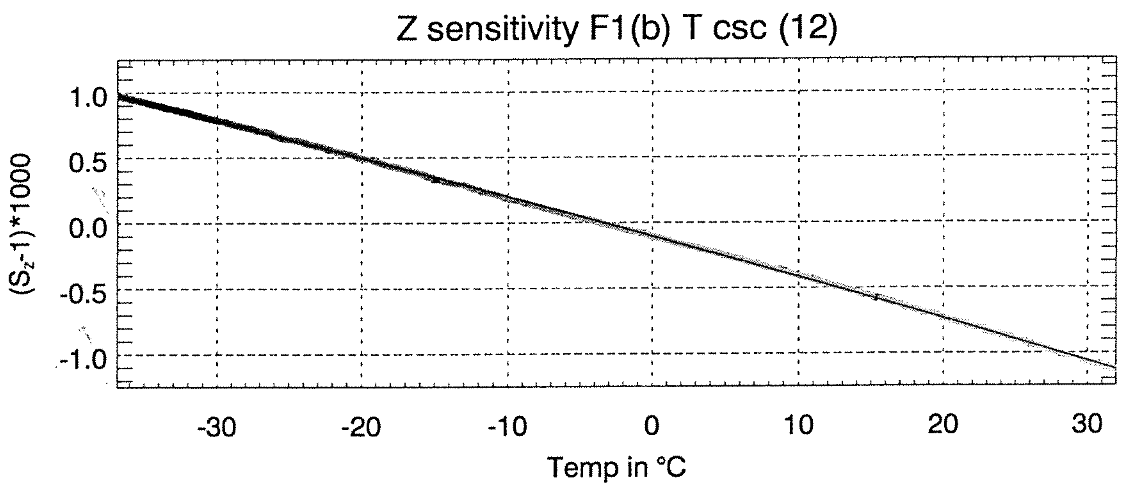

(500), 0.99989731 -3.0735406e-05 -3.9794076e-08

Figure 8-10 CSC 1 , temperature dependence of scale factor

Angle 12 F1(a) T csc (12)

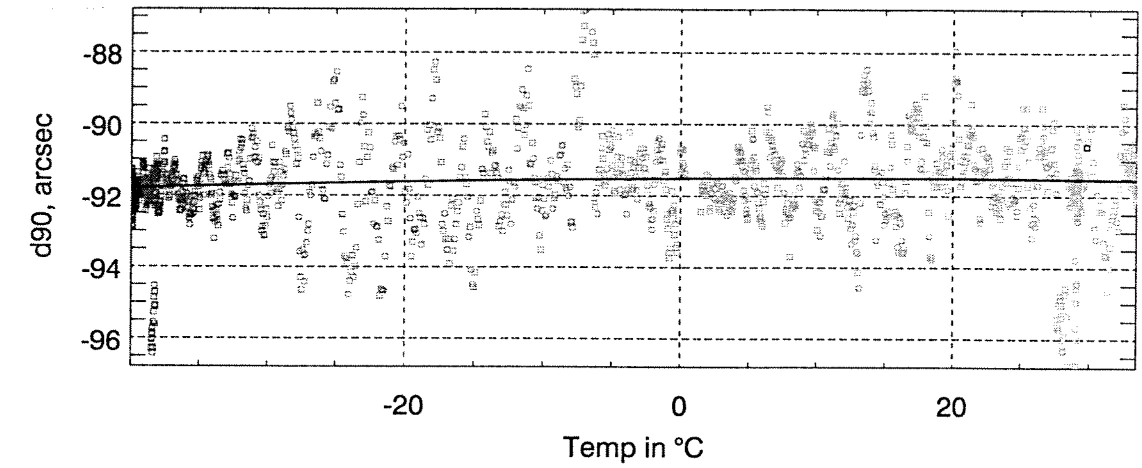

(400), 89.974579 7.7694791e-07 -2.9822176e-08

Angle 13 F1(a) T csc (12)

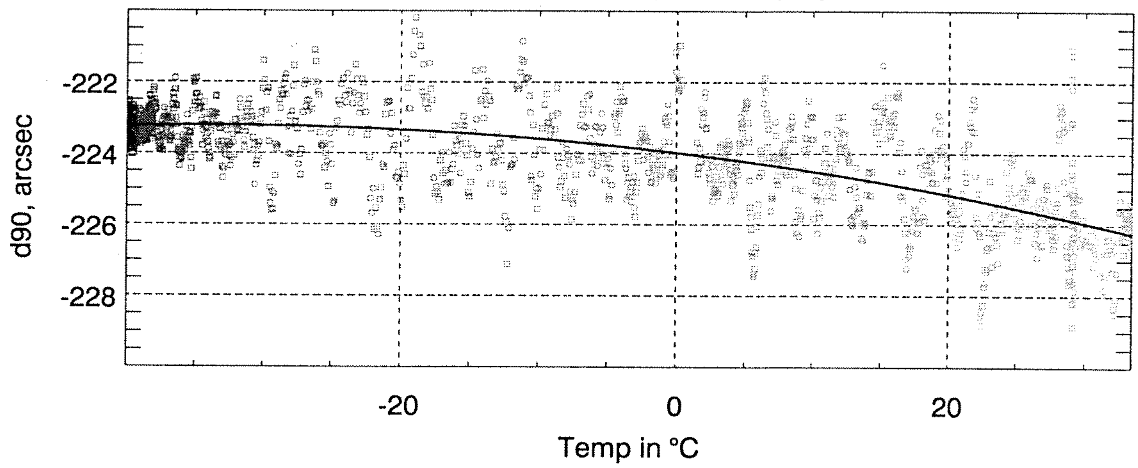

(400), 89.937783 -1.2615187e-05 -1.8608553e-07

Angle 23 F1(a) T csc (12)

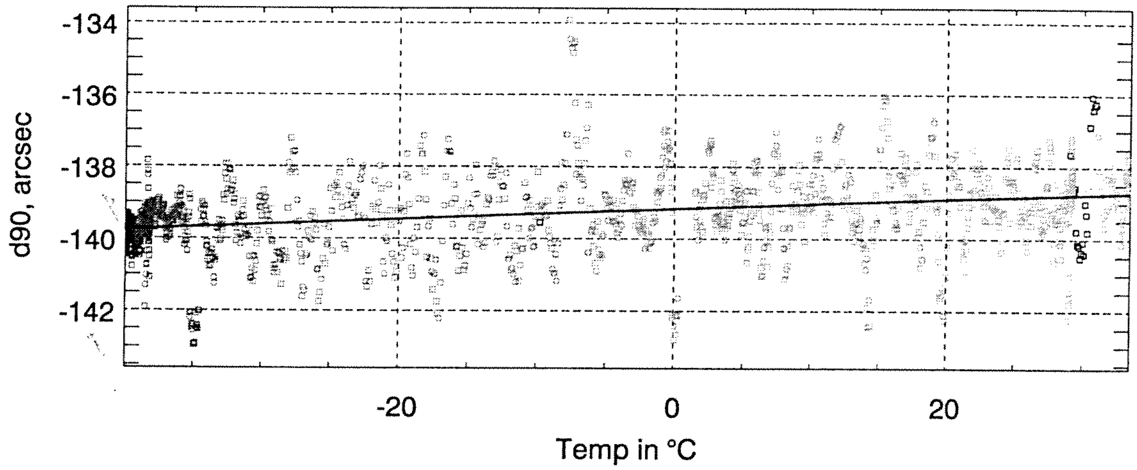

(400), 89.961342 3.8835066e-06 -5.3979784e-09

Figure 8-11 CSC 1 , behaviour of sensor misalignment versus temperature

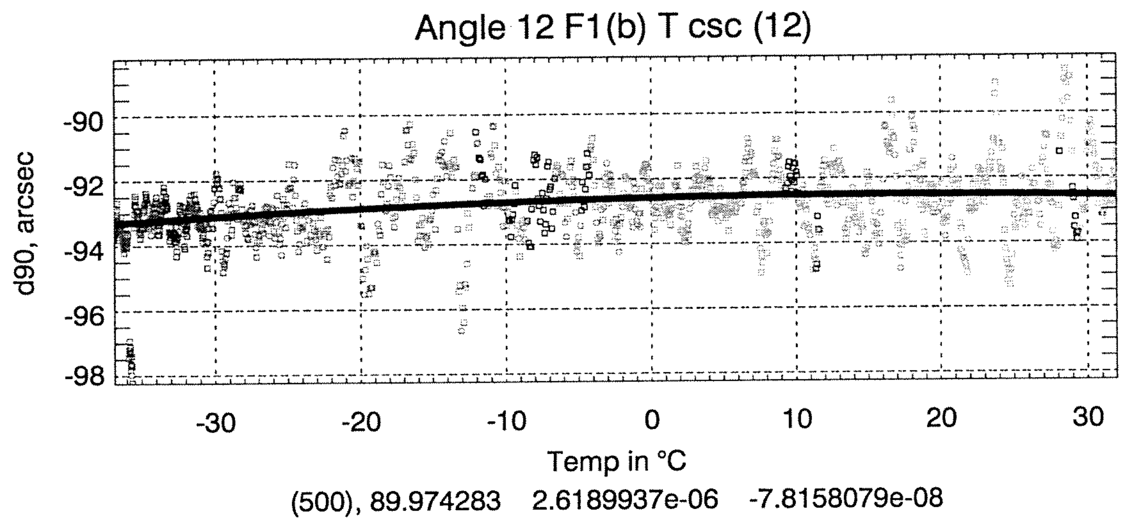

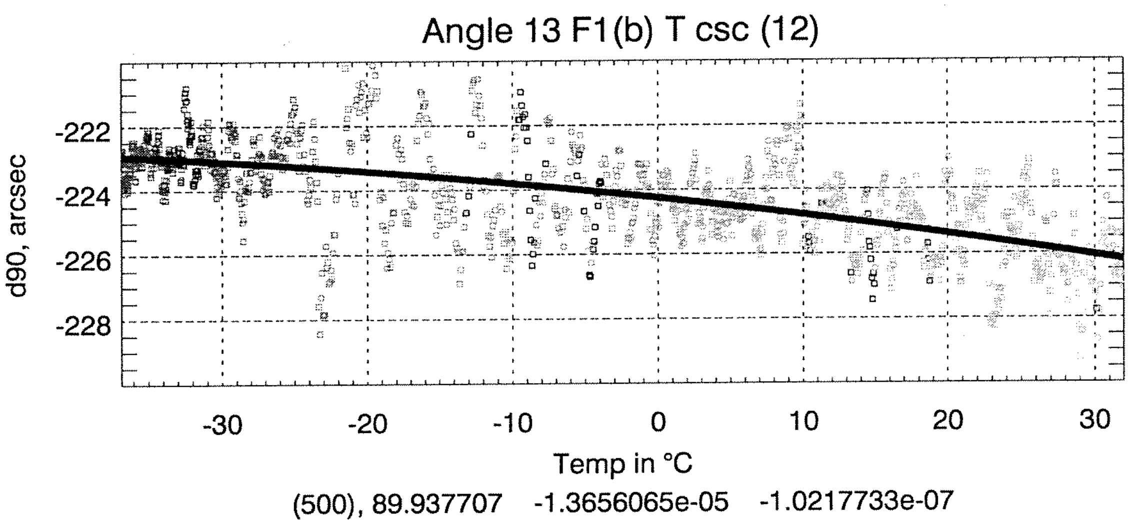

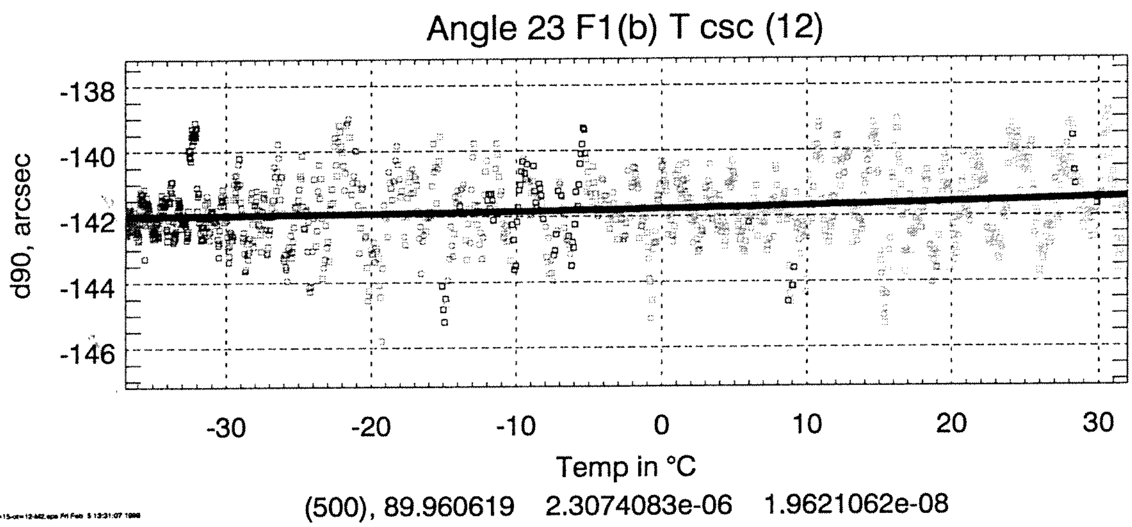

Figure 8-12 CSC 1 , behaviour of sensor misalignment versus temperature

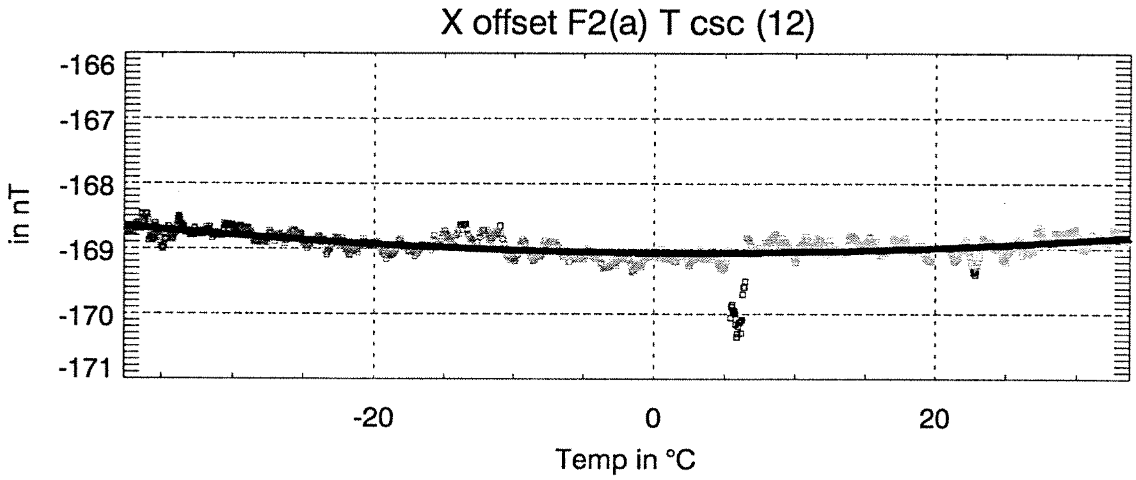

(500), -169.05989 -0.0015757884 0.00025392965 1.4559271e-07

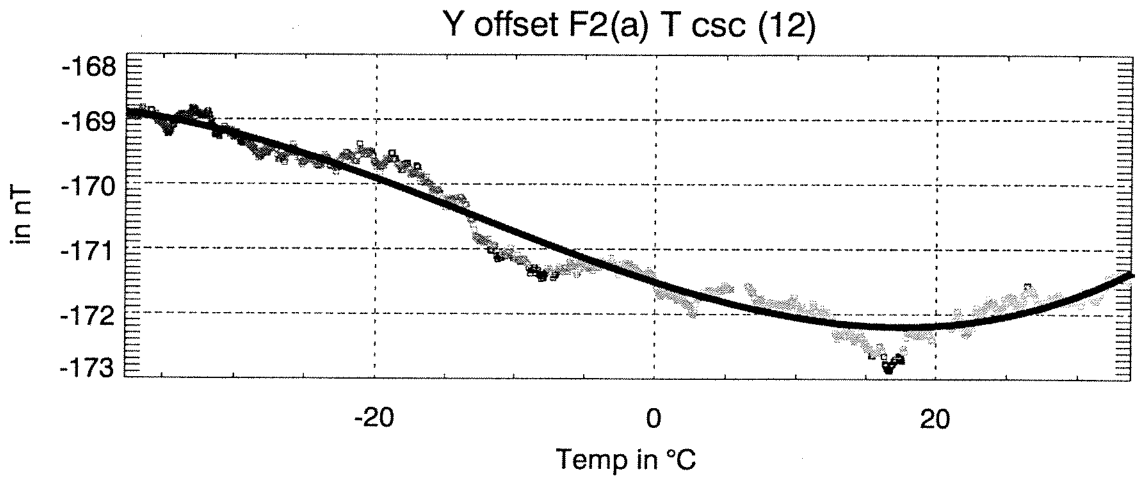

(500), -171.50899 -0.068868008 0.0011593695 3.0343396e-05

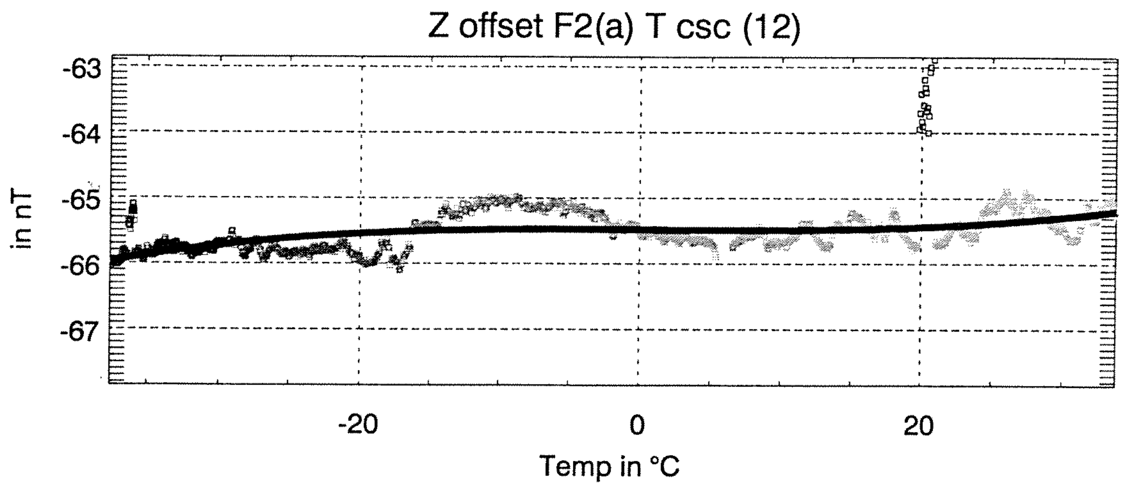

(500), -65.480520 -0.0011697306 -2.6454403e-05 9.3227343e-06

Figure 8-13 CSC 2 , change of offsets versus temperature

X sensitivity F2(a) T csc (12)

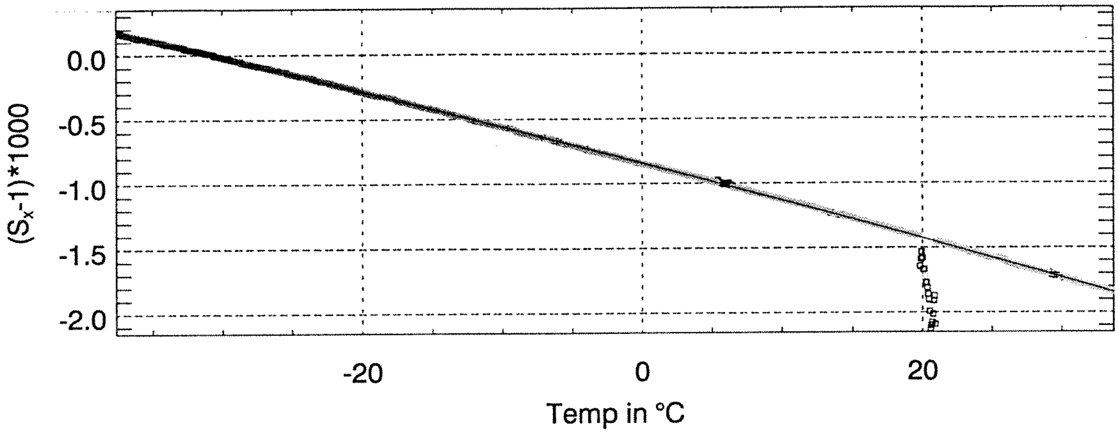

(500), 0.99915934 -2.8460550e-05 -3.8476513e-08

Y sensitivity F2(a) T csc (12)

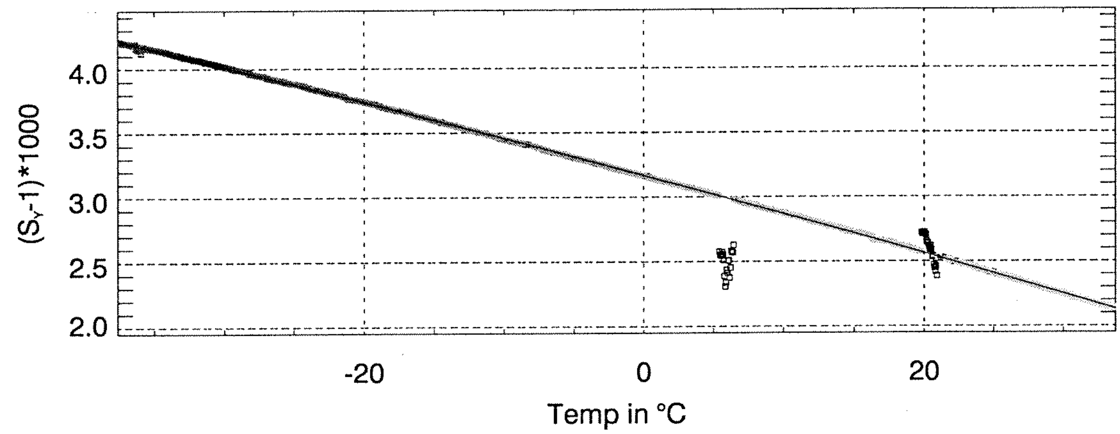

(500), 1.0031678 -2.9400423e-05 -3.9910881e-08

Z sensitivity F2(a) T csc (12)

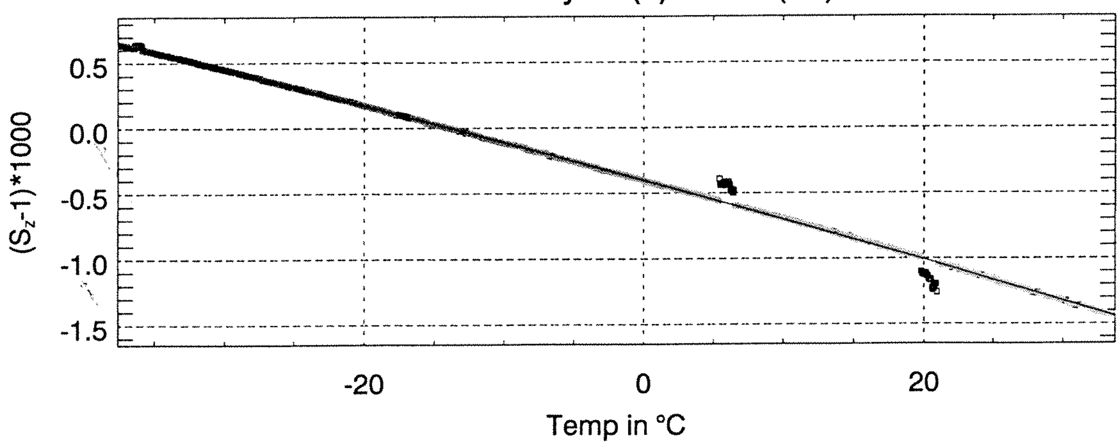

(500), 0.99959889 -2.9514577e-05 -4.0652993e-08

Figure 8-14 CSC 2 , temperature dependence of the scale factor

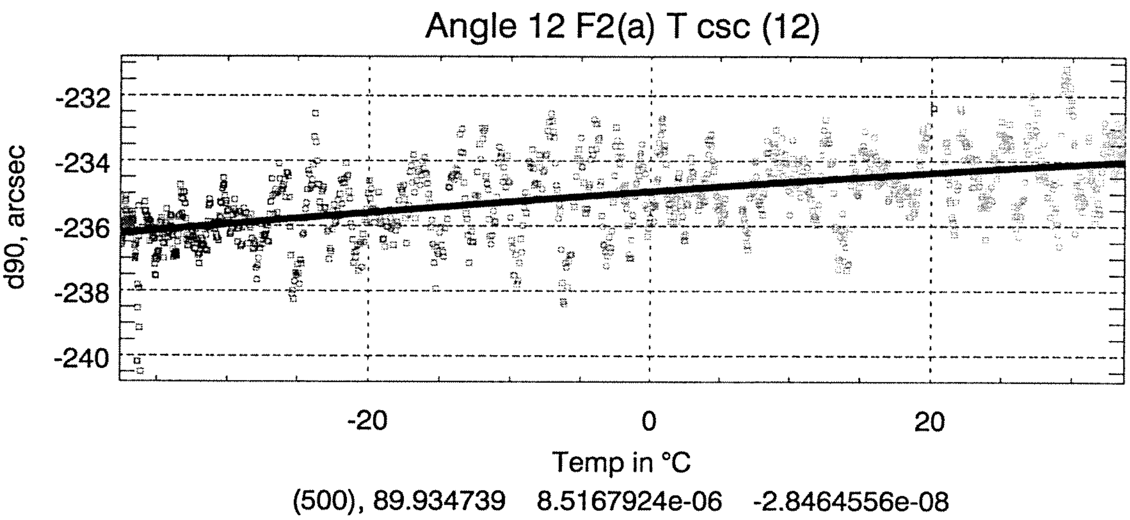

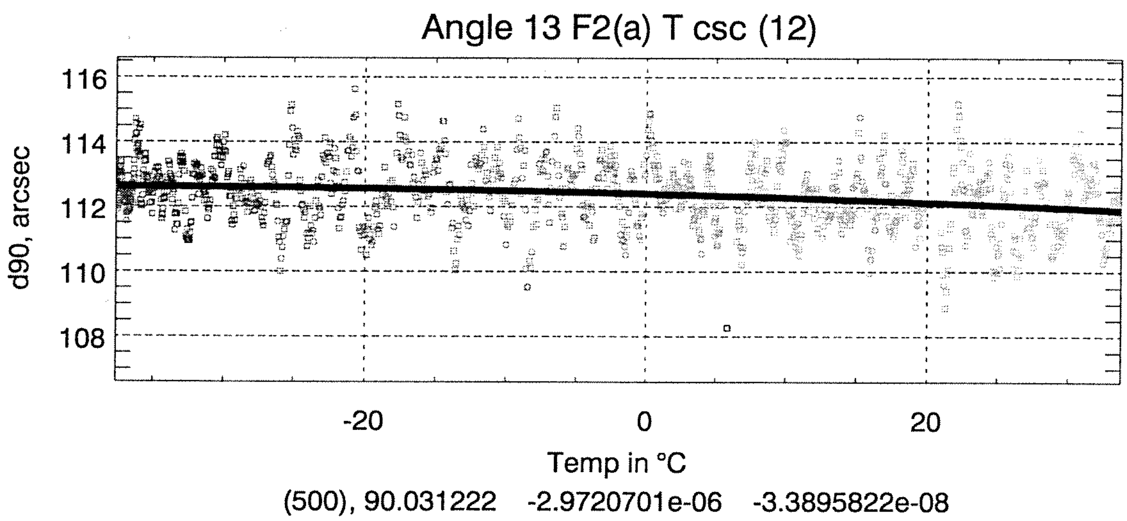

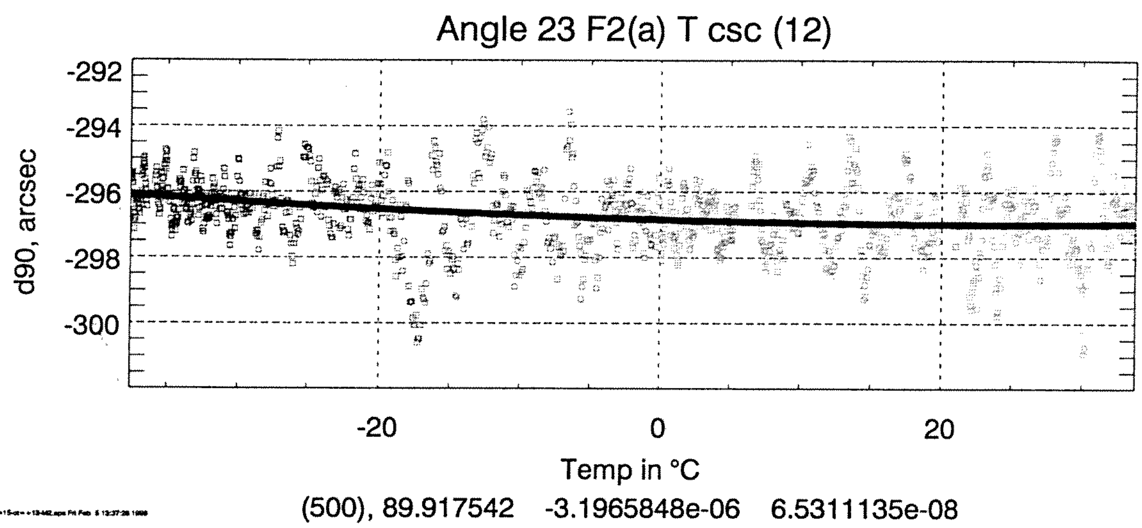

Figure 8-15 CSC 2 , behaviour of sensor misalignment versus temperature

9 SUMMARY

The performance of the CHAMP FGM flight sensors CSC1 and CSC2 was tested in the magnetic facility "Magnetsrode" operated by the Technical University of Braunschweig. The reproducibility and the high resolution of the results can be taken as an indication for the excellent performance and stability of the magnetic facility.

Our primary tool for calibrating the facility was a GEM Overhauser magnetometer. By applying the scalar calibration method to a set of evenly distributed field settings on a constant magnitude shell, we obtained apparently reliable results (low residuals). In addition measurements with the CSC sensor taken at three mutually orthogonal orientations, were combined to solve simultaneously for the facility and the sensor parameters. There are small but significant differences of the order of 5 nT and 10 arcsec in the estimates for the facility parameters. The parameters from the three-tilt calibration provide a much more homogeneous set of results. For ambient temperatures of 16.5°C we derived a new set of parameters which have to be compared to those in section 6.

Scale factors	F_X = 0.99989 nT/EU F_Y = 0.99992 nT/EU F_Z = 0.999965 nT/EU
Offset fields	O_X = -0.6 nT O_Y = -5.3 nT O_Z = -8.2 nT
Angles between components	(X,Y) = 90.0022° (X,Z) = 89.9940° (Y,Z) = 89.9661°

An investigation of the discrepancy between these two methods of calibration will be subject of a test at the magnetic facility of the IABG.

During the presented test the CSC sensors demonstrated their outstanding features. The noise level of the complete magnetometer is below 0.2 nT. There is no indication of a transverse field effect. A slight residual non-linearity of 0.2 nT could be attributed to the analogue/digital converters.

Since the EM magnetometer electronics were used during the test, the obtained sensitivities and offsets are of no concern here. Their determination will be subject of a later test at the IABG facility. The angles between the measuring axes, which can be regarded as finger-prints of the sensors, have been determined. For ambient temperatures (18.5°C) we obtained

	CSC 1	CSC 2
Angles between measuring axes	(X,Y) = 89.9745° (X,Z) = 89.9377° (Y,Z) = 89.9613°	(X,Y) = 89.9347° (X,Y) = 90.0311° (Y,Z) = 89.9173°

These numbers could be reproduced in all runs with an uncertainty of ±1.5 arcsec.

An important part of this test was the calibration of the temperature dependence of the CSC sensor parameters. For both sensors we identified how temperature changes sensitivity, but there is no or only a marginal influence on the offsets and sensor orientations. The actual numbers for 0°C are:

	CSC 1	CSC 2
Offsets	dX_0/dT = negligible dY_0/dT = negligible dZ_0/dT = -0.05 nT/K	dX_0/dT = negligible dY_0/dT = -0.05 nT/K dZ_0/dT = negligible
Sensitivities	$dS_X/dT = -29.60 \cdot 10^{-6}/K$ $dS_Y/dT = -30.37 \cdot 10^{-6}/K$ $dS_Z/dT = -30.46 \cdot 10^{-6}/K$.	$dS_X/dT = -28.45 \cdot 10^{-6}/K$ $dS_Y/dT = -29.38 \cdot 10^{-6}/K$ $dS_Z/dT = -29.50 \cdot 10^{-6}/K$
The quadratic terms for all three components	$-3.8 \cdot 10^{-8}/K^2$	$-3.9 \cdot 10^{-8}/K^2$
Angles between axes	d(X,Y)/dT = negligible d(X,Z)/dT = $-1.3 \cdot 10^{-5}$deg/K d(Y,Z)/dT = negligible	d(X,Y)/dT = negligible d(X,Z)/dT = negligible d(Y,Z)/dT = negligible

Because of the rather large temperature coefficient of the sensitivity great care has to be taken that this effect does not deteriorate the measurements. If the temperature change rates exceed 1 K/h the phase shift of the response between the thermistors and the sensor feed back coils have to be taken into account. In this test we found that the T_{CSC} readings are leading the coil response by 8 min and the T_{sens} are lagging it by 8 min. These time shifts are probably depending on the thermal environment of the CSC and thus have to be confirmed in space during the commissioning phase.

The results obtained during the test demonstrate that the FGM sensors fulfil their specified performance.

10 APPENDIX A

CHAMP Mag. Calibrat. of FGM in M'rode 23. March 1998
Test run CSC F1 A:\CHF1-601.cal

Misalignment angles in deg.	xy = 90.0031	xz = 89.9962	yz = 89.9664
Facility scale factors in nT/0.1 mV	0.99988	0.99993	0.99994
Facility offsets in nT	2.00	-2.20	-1.20
Number of data set	1		
Parameters in EU	1.000991	1.202127E-02	1.746618E-03
	-1.159088E-02	0.9981528	-4.63988E-03
	-6.708939E-04	5.286726E-03	1.00067
	-165.9088	-157.4271	-77.58798
Sensor reference temperature:	18.5 °C		
Sensitivities in nT/EU	0.9989426	1.001764	0.9993179
Offsets in nT	-165.73	-157.70	-77.54
Misalignment (1,2), (1,3), (2,3); in arcsec	95	233	140
in degree	89.9736	89.9353	89.9610

Step	Applied fields, nT			Residuals , nT		
	X	Y	Z	X	Y	Z
1	-54214.43	11508.60	-22960.84	-0.23	0.02	-0.18
2	-40704.14	11924.98	-42424.99	-0.04	0.04	-0.01
3	35687.39	-22962.60	-42425.06	-0.09	-0.06	0.10
4	-27706.93	-47991.26	22958.27	-0.20	-0.01	-0.05
5	-22959.25	55426.47	-1.53	-0.18	-0.08	-0.19
6	-44838.66	32591.41	22958.28	-0.07	0.06	-0.10
7	-40697.46	-11929.70	42422.40	-0.12	0.08	-0.23
8	-44841.68	32564.50	-22961.00	-0.06	0.09	0.00
9	17133.96	-52704.41	22958.24	-0.16	0.21	0.08
10	-54211.69	11535.56	22958.24	-0.34	0.13	0.07
11	37092.86	-41180.16	22958.19	-0.35	0.13	0.21
12	-5790.44	-55140.55	-22960.96	0.00	0.09	0.12
13	17125.03	52700.36	-22960.99	0.02	0.03	0.09
14	5.23	-59997.66	-1.66	-0.06	-0.11	0.08
15	-44837.94	-32595.97	-22960.86	-0.12	-0.10	0.02
16	11476.47	19848.88	-55430.62	-0.14	-0.04	-0.05
17	35684.76	22908.82	-42425.11	-0.02	0.15	-0.05
18	-27776.98	32083.96	42422.45	-0.16	0.09	-0.23
19	5.94	33.75	59994.97	0.00	-0.10	0.01
20	37089.61	-41206.85	-22961.02	-0.11	-0.08	0.11
21	17629.04	-38566.86	42422.47	0.08	0.05	-0.11
22	-1.69	59993.48	-1.63	0.04	-0.43	0.04
23	17130.66	-52731.37	-22960.91	0.08	0.08	0.04
24	22963.50	31.31	55427.93	-0.06	-0.19	0.35
25	-5793.37	55136.21	22958.24	-0.15	-0.06	0.11
26	-40702.59	-11979.19	-42425.22	-0.15	-0.09	0.15
27	11483.54	19913.62	55427.93	-0.14	0.07	0.18
28	22957.08	55426.52	-1.69	-0.11	-0.08	0.06
29	-5796.27	55109.57	-22960.99	-0.04	-0.13	0.17

30	11478.45	-19918.06	-55430.68	0.12	0.04	0.17
31	-11479.64	-19918.02	-55430.70	-0.08	-0.10	0.11
32	-59990.34	-2.54	-1.67	-0.20	-0.10	-0.10
33	-27715.17	47986.98	-22960.93	0.01	0.16	-0.07
34	-44835.11	-32569.01	22958.30	-0.27	-0.03	-0.09
35	22963.14	-55430.70	-1.62	-0.13	0.14	0.00
36	-55422.48	-22961.73	-1.52	-0.08	-0.05	-0.12
37	55429.23	12.32	22958.11	-0.17	-0.02	0.09
38	-11482.01	19848.87	-55430.58	0.36	0.02	-0.03
39	-27712.06	48013.95	22958.17	0.17	0.13	0.02
40	-11474.83	19913.60	55428.01	0.39	0.12	0.21
41	42420.23	-25.99	-42425.08	0.05	0.02	-0.04
42	-11472.75	-19853.22	55427.99	0.46	-0.06	0.28
43	42425.25	-42425.25	-1.61	0.18	-0.07	-0.06
44	17625.08	38612.24	42422.43	0.13	-0.13	-0.20
45	59994.12	-1.11	-1.61	-0.19	-0.10	-0.20
46	55426.39	-14.58	-22960.88	-0.13	-0.13	-0.17
47	-27710.04	-48017.97	-22960.96	0.22	-0.06	0.12
48	55428.96	-22961.43	-1.54	0.02	-0.05	-0.17
49	-54213.50	-11539.94	-22960.84	0.22	-0.19	-0.10
50	37085.54	41176.11	-22960.96	-0.07	-0.20	-0.06
51	22956.66	-33.40	-55430.53	0.00	-0.18	-0.11
52	17623.76	-38616.28	-42425.16	0.01	-0.08	-0.01
53	-27773.44	-32038.85	42422.54	0.05	-0.09	-0.33
54	11485.65	-19853.15	55428.12	0.19	-0.31	-0.01
55	-6034.92	42014.05	42422.63	0.06	-0.30	-0.22
56	-5787.27	-55113.70	22958.40	-0.06	0.06	-0.02
57	-22953.04	-55430.83	-1.59	-0.16	0.05	0.02
58	37088.29	41202.93	22958.22	-0.14	-0.14	0.11
59	-22952.73	29.73	55428.06	0.23	0.10	0.33
60	-1.73	-36.29	-59997.56	0.02	0.05	0.25
61	42425.63	23.52	42422.54	0.04	0.11	-0.22
62	-27782.42	32034.37	-42425.02	0.27	0.11	0.13
63	-55424.97	22957.08	-1.57	-0.10	0.10	-0.05
64	35690.46	22958.47	42422.48	-0.13	0.06	-0.19
65	17128.12	52727.01	22958.28	0.07	0.17	0.21
66	-42416.84	-42425.49	-1.56	0.00	0.17	0.11
67	-42421.45	42421.18	-1.46	0.00	-0.05	0.06
68	50636.24	22556.36	22958.21	-0.01	0.29	-0.01
69	-6035.97	-42018.27	-42424.98	0.16	0.08	0.02
70	50638.45	-22533.77	22958.15	0.11	0.19	-0.06
71	55426.56	22957.22	-1.61	-0.07	0.11	-0.07
72	-6030.69	-41968.88	42422.33	0.33	0.03	-0.14
73	-40698.65	11974.66	42422.50	0.32	0.03	-0.07
74	42420.88	42421.23	-1.65	-0.18	-0.06	0.03
75	17619.62	38562.87	-42425.00	0.13	-0.17	0.08
76	-6040.39	41964.60	-42425.11	0.20	-0.04	0.13
77	-22959.77	-34.84	-55430.61	0.14	0.17	0.07
78	50633.16	22529.41	-22961.01	0.11	0.26	-0.12
79	50635.68	-22560.36	-22961.00	0.20	0.10	-0.19
80	-27779.02	-32088.25	-42425.06	0.11	0.12	-0.16

11 APPENDIX B

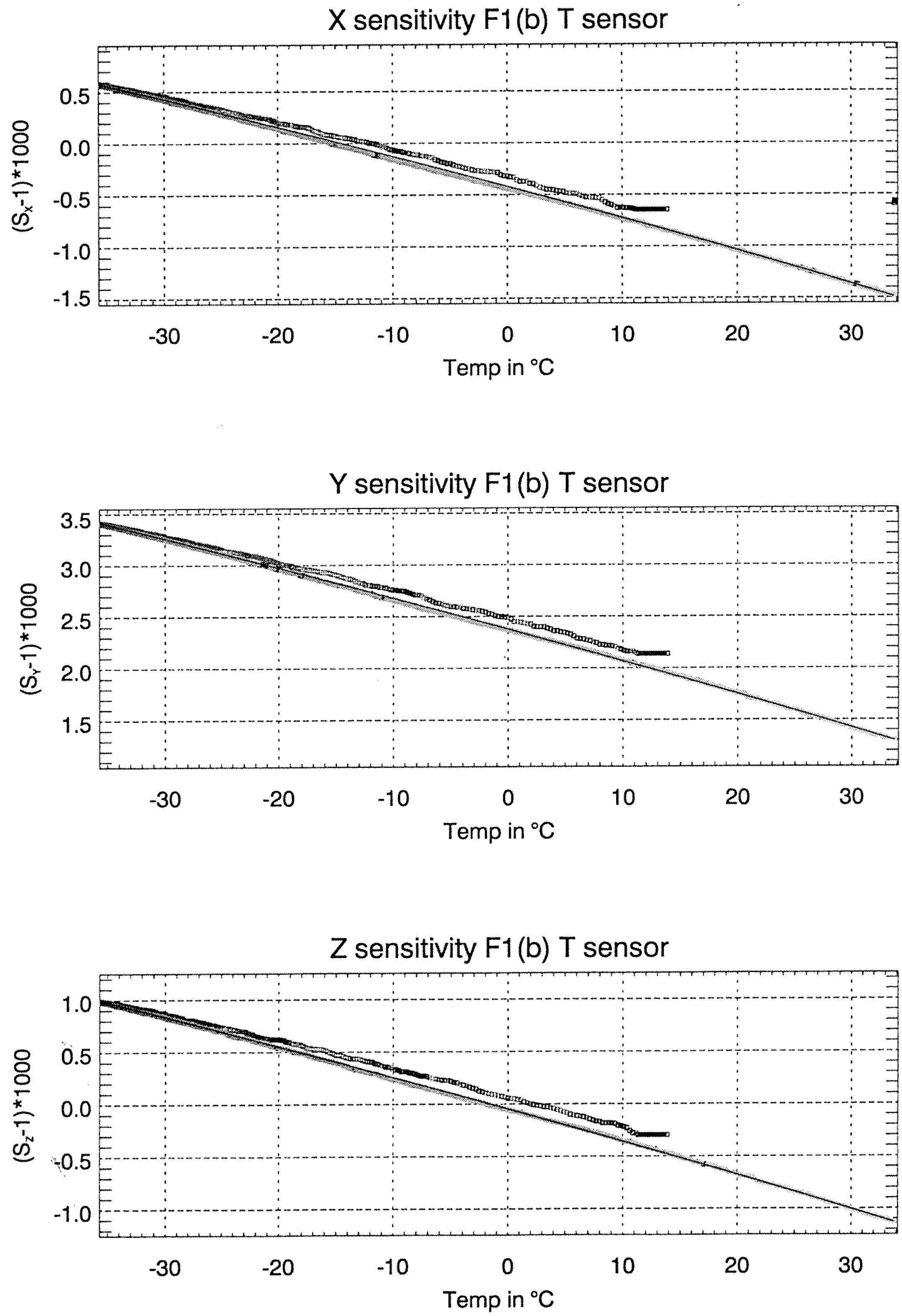

Figure 11-1 Change of scale factors versus T_{SENS} readings

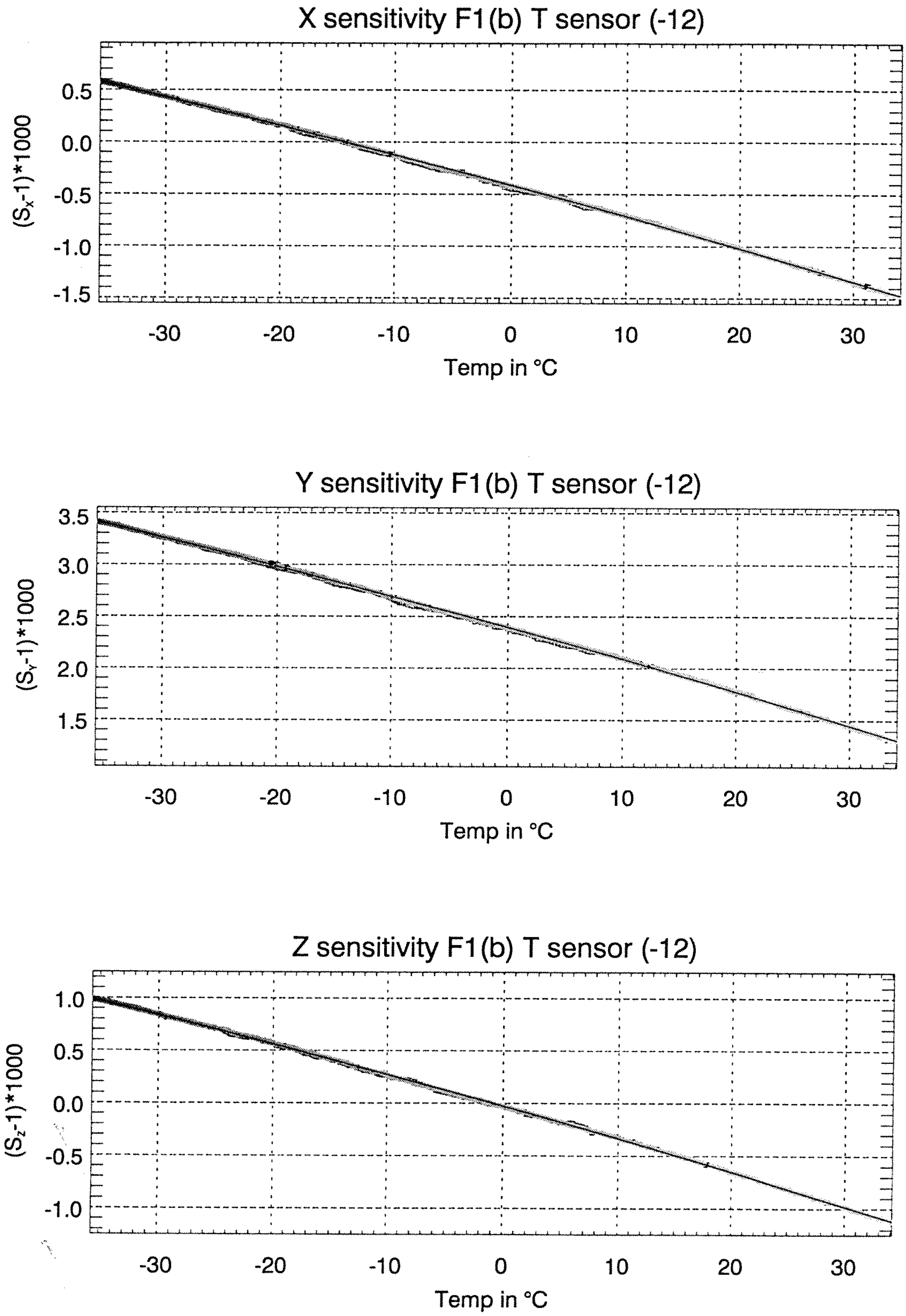

Figure 11-2 Change of scale factor versus temperature T_{SENS} readings advanced by 8 minutes

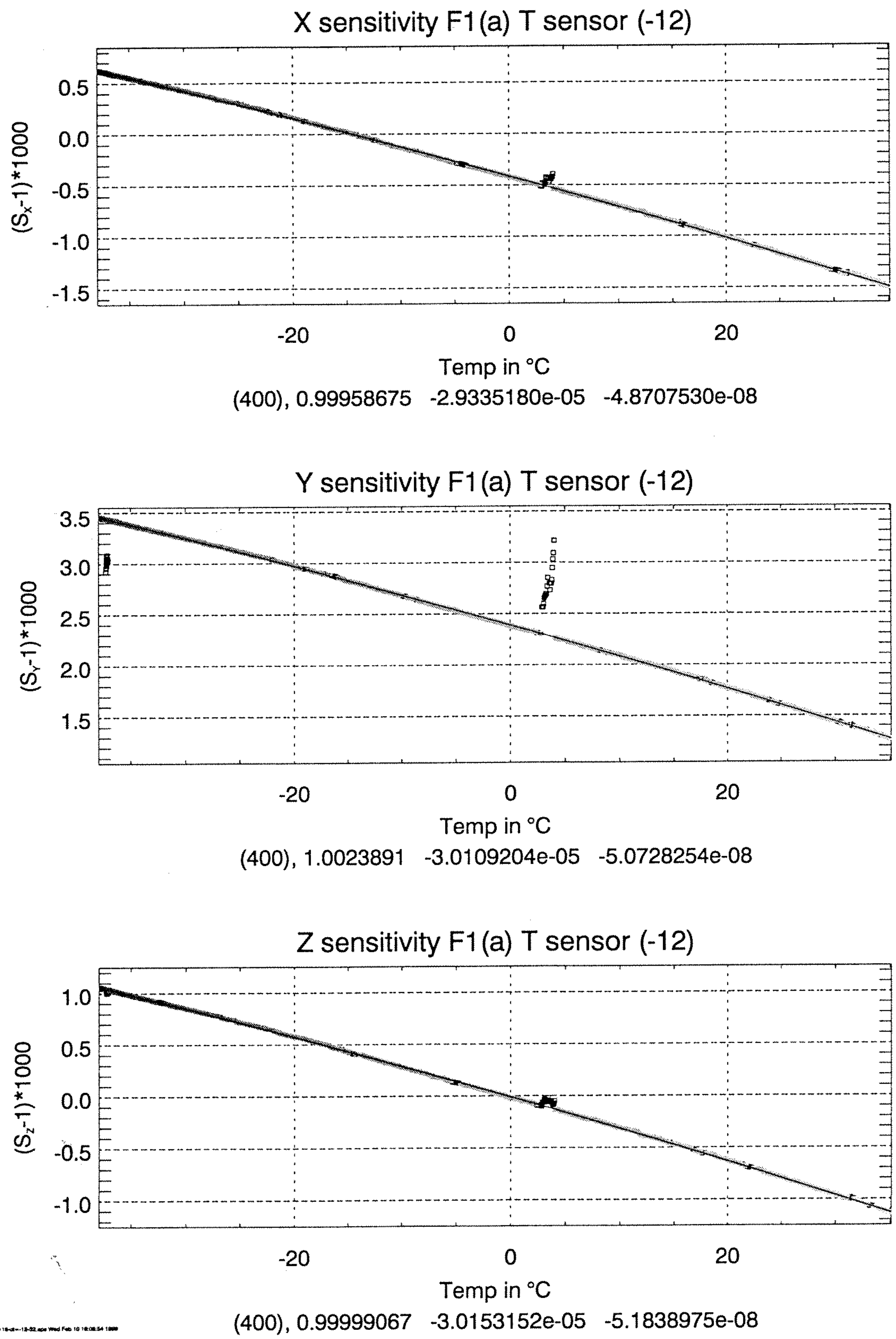

Figure 11-3 CSC 1 , change of scale factors versus sensor temperature (T_{SENS})

X sensitivity F1(b) T sensor (-12)

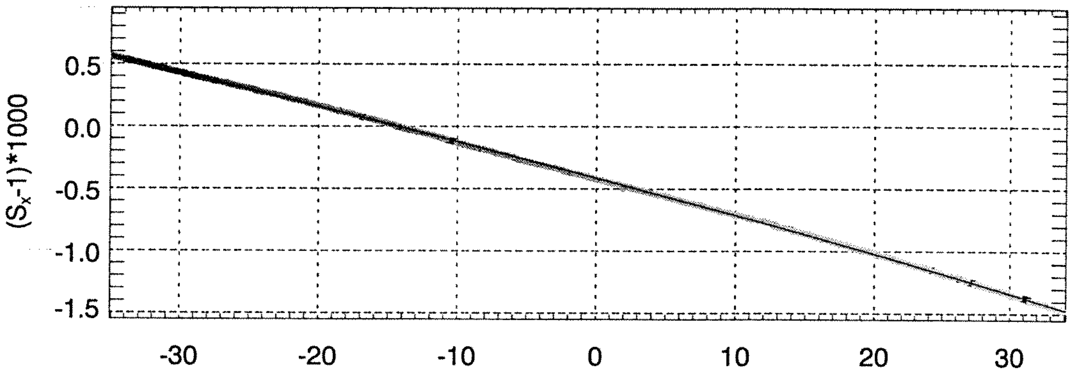

(500), 0.99958678 -2.9514095e-05 -4.5857174e-08

Y sensitivity F1(b) T sensor (-12)

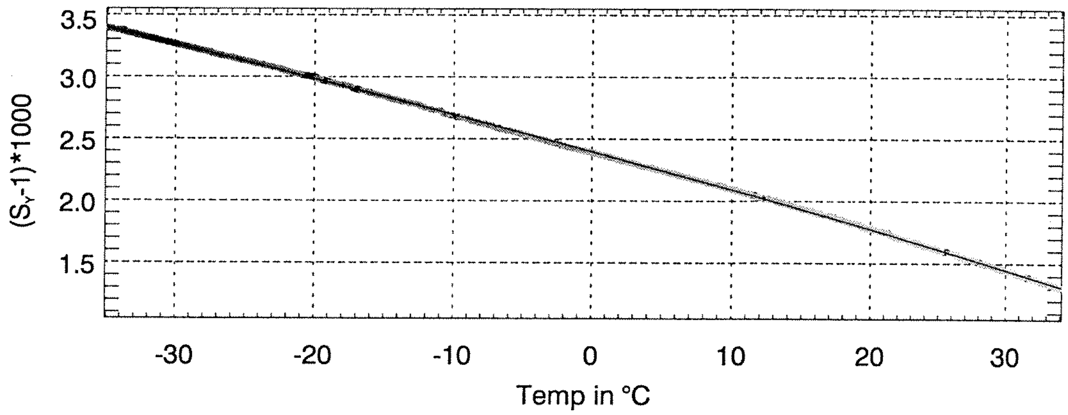

(500), 1.0023973 -3.0255162e-05 -4.7436864e-08

Z sensitivity F1(b) T sensor (-12)

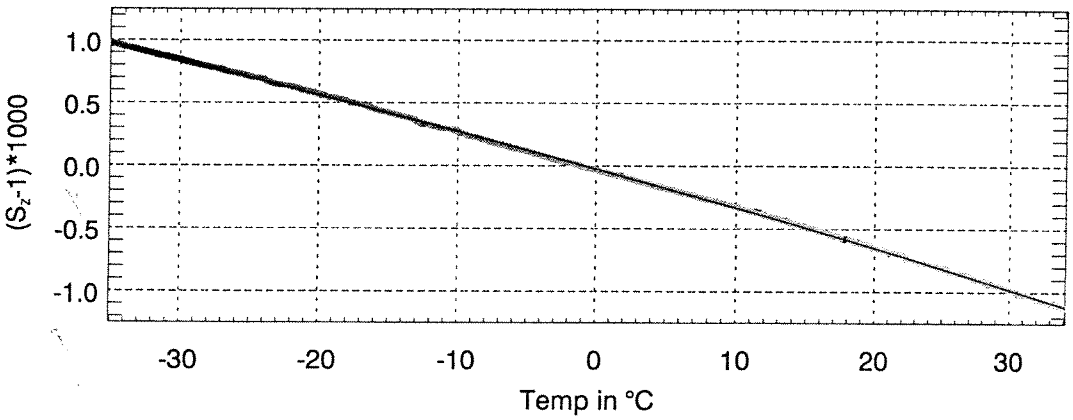

(500), 0.99997496 -3.0363066e-05 -4.9742351e-08

Figure 11-4 CSC 1 , change of scale factors versus sensor temperature (T_{SENS})

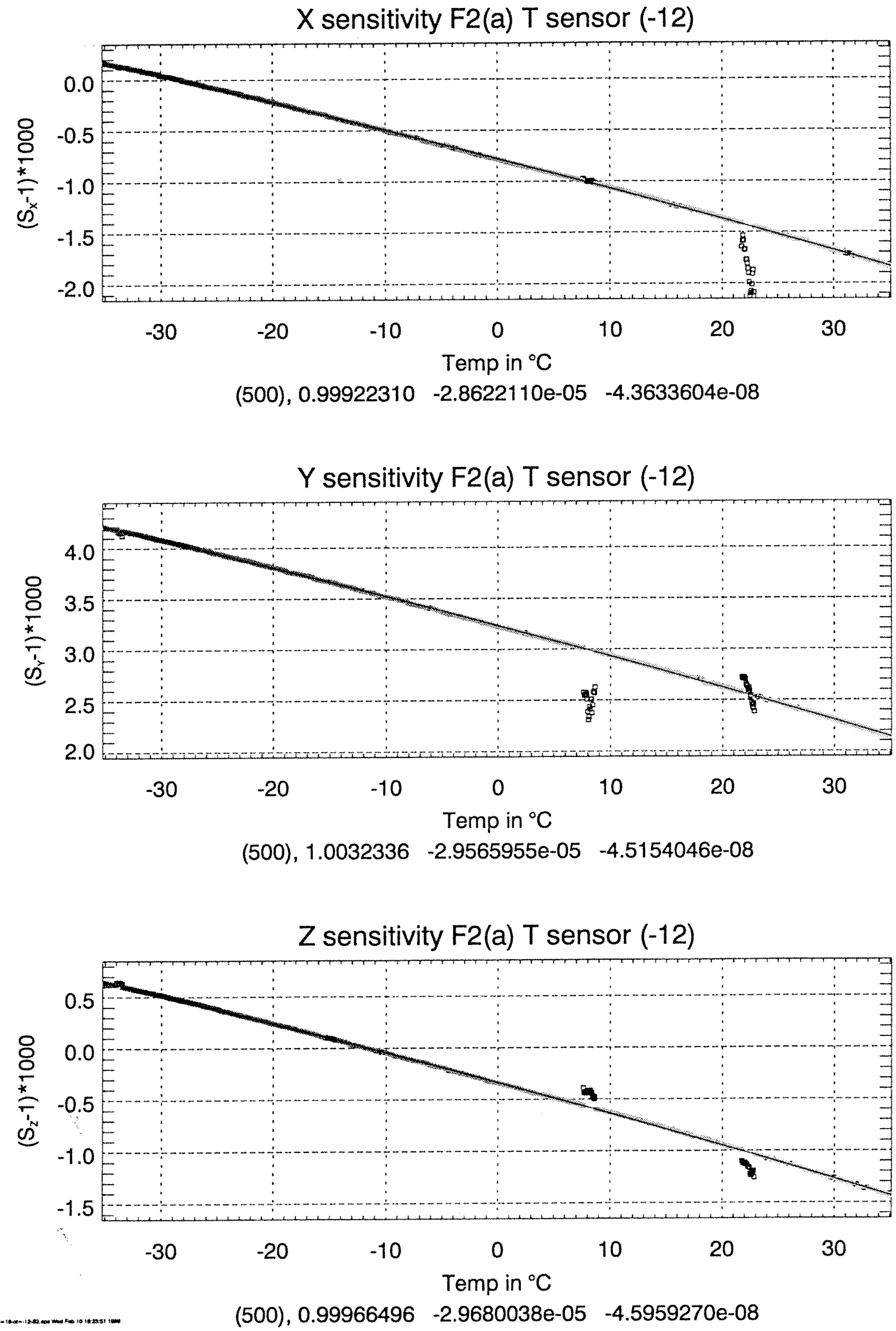

Figure 11-5 CSC 2 , change of scale factors versus sensor temperature (T_{SENS})